

# Deep-water seafloor geomorphic features of the Santos Basin, Southeastern Brazilian Margin, shown by analyses and integration of an extensive 3-D seismic data set

Cízia Mara Hercos<sup>1\*</sup>, Simone Schreiner<sup>2</sup>, Eugênio Taira Inácio Ferreira<sup>2</sup>

<sup>1</sup> PETROBRAS - Centro de Pesquisas Leopoldo A. Miguez de Mello - Universidade Federal do Rio de Janeiro (Av. Horácio de Macedo, 950 - Cidade Universitária - CEP: 21.941-915 - Rio de Janeiro - RJ - Brazil).

<sup>2</sup> PETROBRAS E&P SUB/ES/GEO - Marine Geology Group (Av. Henrique Valadares, 28 - Centro - CEP: 20.231-030 - Rio de Janeiro - RJ - Brazil).

\* Corresponding author: [cizia@petrobras.com.br](mailto:cizia@petrobras.com.br)

## ABSTRACT

The extensive coverage of 3-D seismic data on the Santos Basin deep water offered an integrated vision of the local physiography and medium- to small-scale geomorphological features, which enhances the understanding of its constructive/deconstructive natural processes and their interrelations. The Santos Basin is a divergent marginal basin composed of three main physiographic provinces: its continental shelf, continental slope, and the São Paulo Plateau, whose dimensions, orientation, gradients, and relief interact with oceanographic, biological, and geological processes. This study geologically contextualized environmental data related to the Regional Environmental Characterization Project of the Santos Basin (hereinafter referred to as PCR-BS), especially regarding the regional physiographical architecture and deep-water geomorphological provinces as a background for the benthic communities and the distribution of several of its geochemical parameters. The integrated analysis of 3-D seismic and multibeam bathymetric data and its derivatives (gradient and edge maps) — calibrated by 108 piston cores — aimed to evaluate its seafloor physiographic features and geological processes. Edge detection seismic attributes enhance gradient contrast, which, in turn, can map innumerable medium- to small-scale geomorphic features (features solved in maps at a 1:1,000,000 scale or larger), such as canyons, channels, ravines, pockmark units, pockmark fields, lineaments, carbonate and coral mounds, salt-related features (crests, minibasins, and crestal grabens), scars and rugous relief associated with mass-transport deposits, and bottom current-related features (depressions and furrows). The slope and the gently dipping plateau (São Paulo Plateau) that follow it eastward show four geomorphological domains based on their direction, profile, average gradient, shelf break isobath, distribution of its medium-small scale geomorphic features, and the presence or absence of evaporites at subsurface. The central-northern São Paulo Plateau contains salt-related topographic elevations (salt diapirs and walls) and depressions (minibasins) that give a rough aspect to the seafloor relief.

**Descriptors:** Seafloor Geomorphology, Seafloor Deposits, Near-surface Seismic Features, Multibeam Bathymetry, 3D Seismic Data

## INTRODUCTION

This study aims to describe the physiography of the Santos Basin and to identify and map its set

of deep-water seafloor geomorphological features by new comprehensive 3-D seismic data and some data analyses of a large high-resolution data base of the Santos Basin uppermost sedimentary section that have been developed in the last 15 years, which found and proposed the existence of major regional domains characterized by dominant geomorphological processes.

Submitted: 31-May-2022

Approved: 30-Oct-2023

Associate Editor: Renato Carreira



© 2023 The authors. This is an open access article distributed under the terms of the Creative Commons license.

This study especially aimed to highlight this geological framework to contextualize the Regional Environmental Characterization Project of the Santos Basin (PCR-BS) environmental data and analyses in several studies of this special issue.

The study area lies in the southeastern Brazilian margin (offshore Paraná, São Paulo, and Rio de Janeiro States) and comprises the continental slope and the São Paulo Plateau provinces of the Santos Basin (Figure 1).

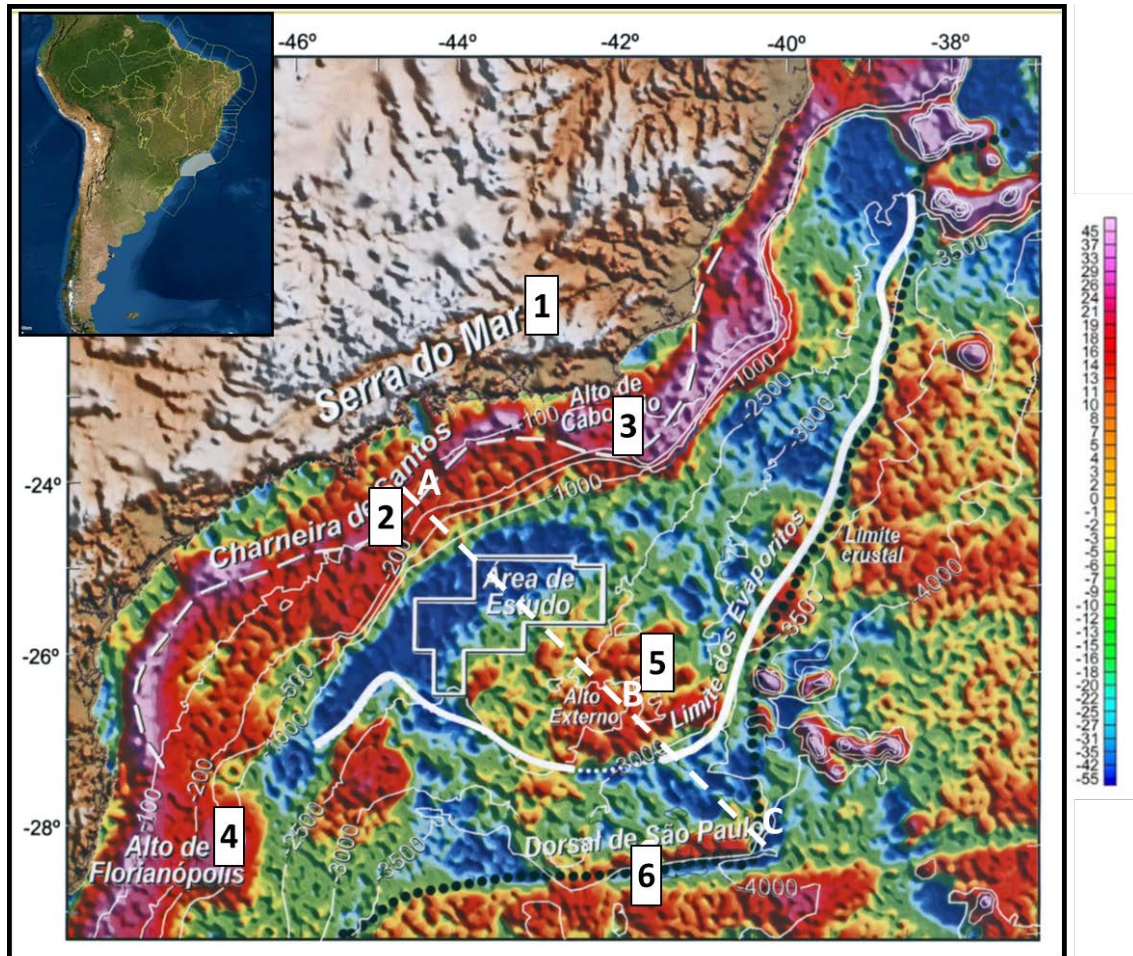


**Figure 1.** Main geological features of the Santos Basin over a composite mosaic with satellite topographic data and free-air gravimetric values (Gamboa et al., 2008, data source: [http://topex.ucsd.edu/cgi-bin/get\\_data.cgi](http://topex.ucsd.edu/cgi-bin/get_data.cgi)). 1- Serra do Mar Range, 2- Cretaceous (Aptian) Hinge Line, 3- Cabo Frio High, 4- Florianópolis High, 5- External High, 6- São Paulo Ridge, ABC- Approximate location of the geological section in Figure 2. Dotted black line- crustal limit, continuous white line- evaporite limit. Colored scale in mgal.

The interpretation of 3-D multichannel seismic and high-resolution geophysical data (which are more restricted) found and mapped physiographic variations and small- and medium-scale geomorphological features and fostered the discussion of a connection with related geological, oceanographic, and biological processes. The systematic seafloor sediment sampling and dating conducted by Petrobras (mainly piston

cores) over decades calibrated the indirect geophysical interpretation and showed that the local geomorphology offers a view of the basin evolution history at least from the Late Palaeogene to the Quaternary.

Most previous studies of the deep-water Santos Basin have focused on discrete morphological features, such as pockmarks, carbonate ridges, coral mounds, and mass-transport deposits (for

instance, Sharp and Badalini, 2013, Schattner et al., 2016, 2018; Mahiques et al., 2017, 2022; Maly et al., 2019; Ramos et al., 2019), assessing localized areas or the impact of oceanic palaeocirculation in the construction of its northeast slope (Duarte and Viana, 2007). This study offers, for the first time, a regional good-resolution 3-D seismic mosaic that provides a broad overview of the morphological feature sets distributed over the continental slope and a large part of the São Paulo Plateau (hereinafter referred to as SPP).

## REGIONAL SETTINGS

The Santos Basin is bounded to the south by the Florianópolis High/São Paulo Ridge, to the north by the Cabo Frio High, to the west by the coastal shoreline, and to the east by the eastern boundary of the SPP. The Santos Basin sedimentary section contains three tectono-stratigraphic sequences above its basement: rift, postrift (or transitional), and drift (Moreira et al., 2007). The uppermost portion of the drift tectono-stratigraphic sequence lies over the continental slope and the SSP. It consists of the Marambaia Formation lithotypes (Maresias Member), which are the target of this study.

According to Souza (1991), the current physiography of the Brazilian margin combines structures inherited from rigid tectonic processes (basement and rift-derived), salt tectonics and sediment reworking by bottom current processes in

deep waters, and shallow-water processes on the continental shelf. In the deep-water Santos Basin, these controls emerge from the correlation of the tectono-stratigraphic-sedimentary events with the current regional physiography and medium-scale bottom geomorphology.

In the Late Cretaceous (Eosantonian), the uplift of the basin western edge relief (Proto Serra do Mar) triggered an intensive progradation of the coastal sediments that lasted up to the end of the Oligocene, which was coeval with the counteregional Cabo Frio Fault (Rowan et al., 2022) formation, the subsequent Albian Gap, and the expulsion of salt toward deep waters (Gamboa et al., 2008). The Cabo Frio fault (Mohriak et al., 1995) is a NE-SW regional antithetic fault that extends for about 400 km from the central compartment of the basin offshore the Santos municipality to the vicinity of the Cabo Frio High to the north.

The ancient deeper depocenter location, which lies under the modern mid-outer continental shelf and slope, suggests continuous subsidence controlled by the Cretaceous Hinge Line and an accommodation space created by eastward salt mobilization, which has resulted in two halotectonic areas: the extensional and compressional (Meisling et al., 2001; Modica and Brush, 2004) or salt-thickened (Jackson et al., 2015) domains (Figure 2), whose different geometries are imprinted on the seafloor geomorphology.

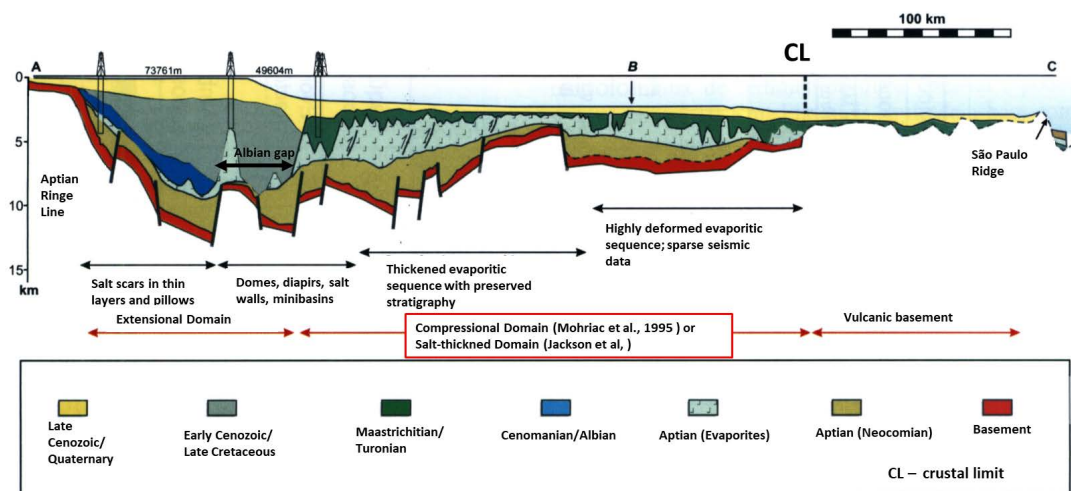


**Figure 2.** Northern/central Santos Basin geological section. The Cretaceous (Aptian) Ridge Line marks the abrupt change in basement dip. The Santos basin depocenter rests under the modern continental shelf and slope (Modified of Gamboa et al. 2008). Section location in Figure 1.

The extensional domain is subparallel to the Cretaceous Hinge line; it is 80-150 km wide and characterized by pillows, domes, and walls with different dimensions and amplitudes (Gamboa et al., 2008). Its eastern boundary almost coincides with the Cabo Frio Fault trace and the Santos Channel, which is situated at a 1500 m water depth. The central and northern Santos Basin shows an abrupt extensional and salt-thickened domain boundary that coincides with the eastward salt base dip change, conditioned by the presence of the underlying external high.

A new uplift episode of the Serra do Mar Ridge and lineament reactivation coeval to volcanisms occurred in the Late Cretaceous-Palaeogene transition, which created the NE aligned pull-apart basin (Taubaté, Resende and Volta Redonda basins) along the Paraíba do Sul fluvial valley, whose course was captured toward the Campos Basin. These events, related to the Continental Rift of Southeastern Brazil installation (Riccomini, 1991), altered the course of the deep-water sedimentation history of the Campos and Santos basins from Late Palaeogene to Recent time. Since the Late Palaeogene, the Campos Basin has received a wide Miocene prograding wedge and important turbidite deposits, whereas the sediment input at the northern Santos Basin was dominated by ocean bottom currents, such as those that constructed the Santos Drift System to the north. However, to the south, fluvial systems continued to flow toward the deep sea during regressive periods. These systems currently consist of the Itajaí-Açu and Ribeira do Iguape rivers.

Duarte and Viana (2007) investigated the impact of oceanic palaeocirculation of the SW Atlantic Ocean in the construction of the Santos Basin northeast slope from the Late Palaeogene to the Quaternary, characterizing variations in bottom current intensity by seismic patterns and physiographical evolution. The authors stated that periods of relative sea-level rise to highstand are related to an increase in drift accumulation, whereas lowstand stages reduced drift sedimentations.

Quaternary glacio-eustatic sea-level variations and ocean bottom currents shaped the slope and SPP of the southeastern Brazilian marginal basins (Souza, 1991; Viana and Faugeres, 1998; Viana et al., 2002). Based on the model proposed by Gardner et al. (2008), we assume that during Quaternary regressive periods (Glacial stages) the deep-water

sedimentation begins with the development a slope apron of mass-transport deposits (cohesive debris flow and/or slump deposits) due to slope failure, which evolve into an effective connection between tributary systems and deep-water with a progressive basin level falling, in which sand transfers effectively build a sand-prone deposition (Turbidite systems) in the lower slope and SPP. In the absence of transfer conduits (Canyons) and well-developed feeder systems (Tributary systems), there predominates hemipelagic deposition and sediments reworking by ocean bottom currents on the slope and SPP.

## DATA AND METHODS

The processed 3-D seismic and high-resolution acoustic geophysical data were supplied by Petrobras and loaded into a computer workstation with a seismic interpretation software (Petrel and Openworks suite) for mapping the geological framework of a seafloor and shallow section (the first 100 m below the seafloor).

The basin bathymetry consists of a mosaic composed of 50 3-D seismic and 44 high-resolution surveys (multibeam bathymetry) and a regional grid provided by the Directorate of Hydrography and Navigation of the Brazilian Navy (DHN) (Figure 3). First, the bathymetric data with different types and resolutions were gridded together with a cell size of 50 m under the least squares method with the following priority: multibeam data (1), 3-D seismic data (2), and DHN regional grid (3). Then, the resulting grid was resampled with a cell size of 100 m.

Seismic data are sampled in time and are usually represented as two-way travel times on a vertical scale. The first reflection related to the seafloor horizon was mapped for each 3-D seismic volume and converted to depth using a water seismic wave propagation velocity equal to 1500 m/s.

The 3D seismic vertical resolution (Tuning thickness) was estimated as from 6 to 10 m at the seafloor horizon using frequency content and the associated wavelet of each 3D seismic data. The tuning effect refers to the variation in the shape of a reflection wavelet created by closely spaced reflecting interfaces, whereas tuning thickness consists of the thinnest interval over which the distance between two closely spaced reflectors can be correctly measured (Lee et al., 2009).

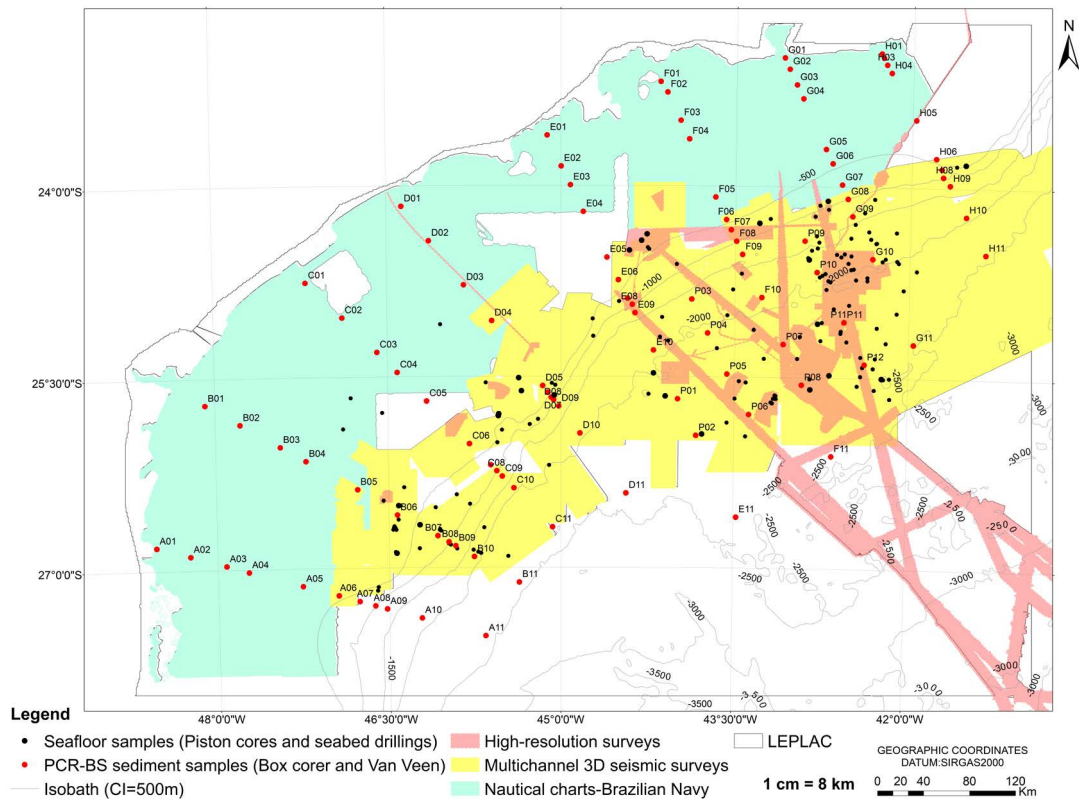


**Figure 3.** Bathymetry map of the Santos Basin showing the different surveys that compound the regional bathymetric mosaic and seafloor sample locations.

Although the detectability or limit of visibility of seafloor features in plain view can be smaller than the tuning thickness, volume definition is limited by this effect (Brown, 2004). Thus, we assume that the seafloor horizon represents a sedimentary layer whose thickness varies from 6 to 10 m.

The gradient and coherence (edge) maps were extracted from the bathymetric grid. Both maps usefully highlighted relief discontinuities, improving the understanding of seafloor morphology (Figure 4). The gradient map was obtained by calculating the arctangent on the first bathymetric derivative grid. The edge detection formula (or Sobel filter) is based on gradient discontinuities and measures how fast pixel values change with the distances in the x- and y-axes (Schreiner et al., 2009).

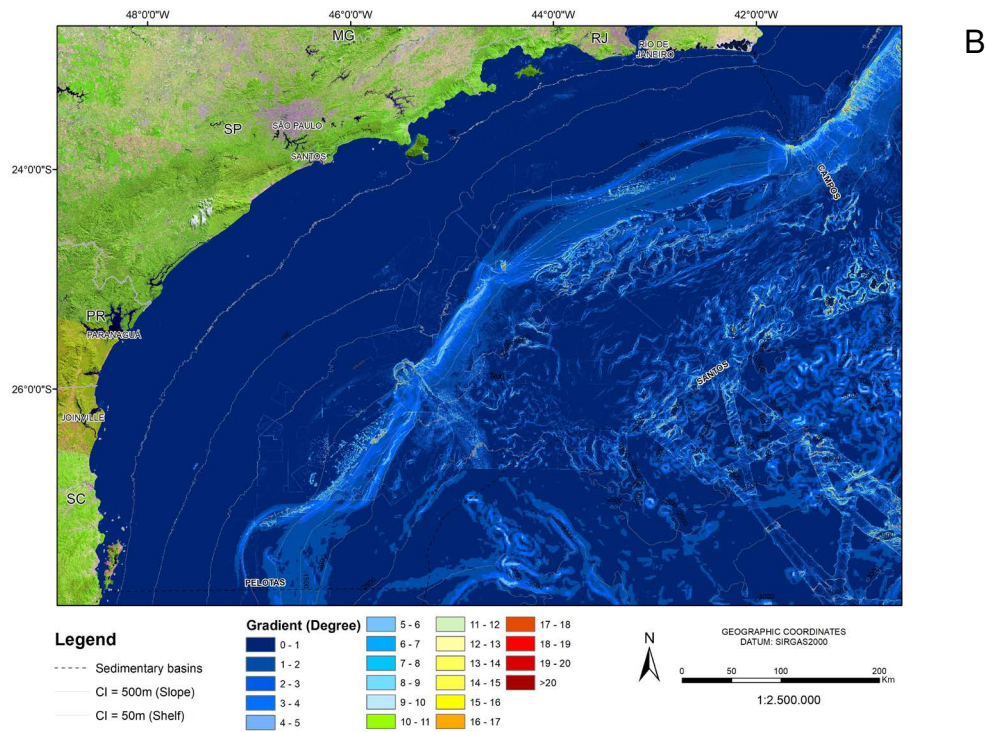
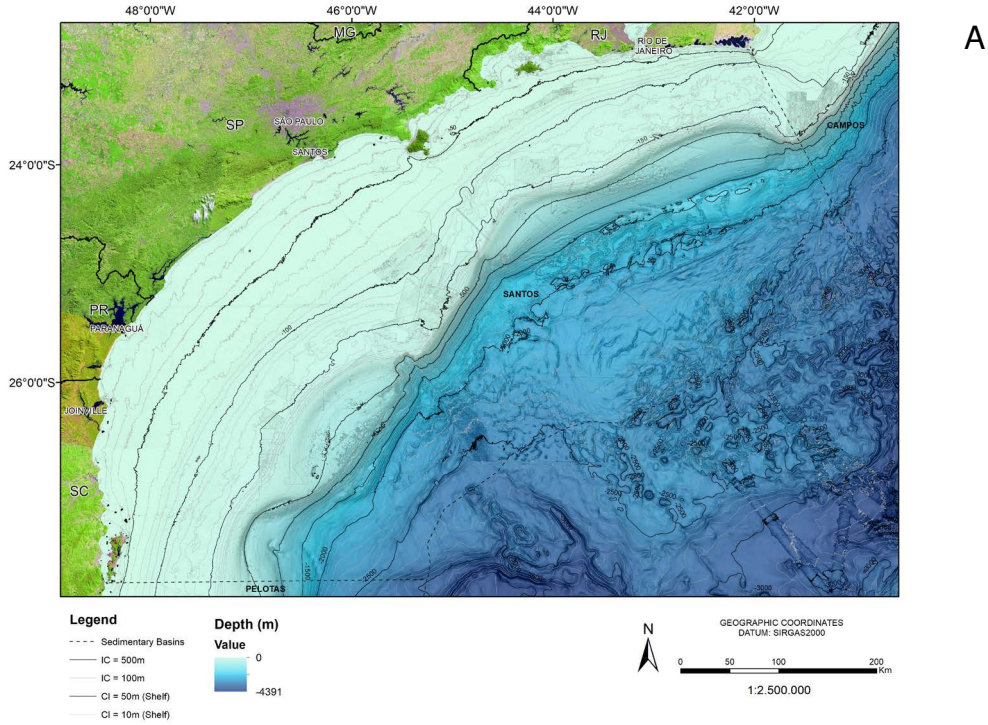
In addition to bathymetry and its derivatives, the analysis of the near-surface seismic reflection patterns (seismic facies) corroborated the interpretation of the surface geomorphological features and its related formation processes. Numerous unpublished internal studies by the

Petrobras marine geology group were compiled and reinterpreted on a scale appropriate for the region. Furthermore, academic studies on the geomorphological features of the Santos Basin were searched, which mainly consisted of detailed descriptions of small areas (for instance, Schattner et al., 2016, 2018; Mahiques et al., 2017, 2022; Maly et al., 2019; Ramos et al., 2019; Duarte and Viana, 2007).

Piston coring for geochemical prospecting and geological-geotechnical surveys provided surface sediment data (108 cores), which were described and dated in many internal Petrobras projects over decades (Figure 3). Climate-dependent foraminiferal biozonation (Ericson & Wollin, 1968), calibrated to the standard oxygen isotopic stages of Imbrie et al. (1985) and refined from Brazilian marginal basin data by Vicalvi (1997), was used to date Upper Quaternary sediments. Most piston cores recovered Holocene drape, which mainly consists of mud, marl, and ooze.

This study assumed that small-scale geomorphic features could be solved in maps at a scale larger than 1:200,000 (for instance, pockmarks units, sediment waves, 3D or 2D bedforms, mass-transport deposits - MTD - with

runouts with hundreds of meters), whereas medium-scale geomorphic features could be represented in maps between 1:200,000 and 1:1,000,000 scales (e.g., mass-transport complexes and pockmarks fields).



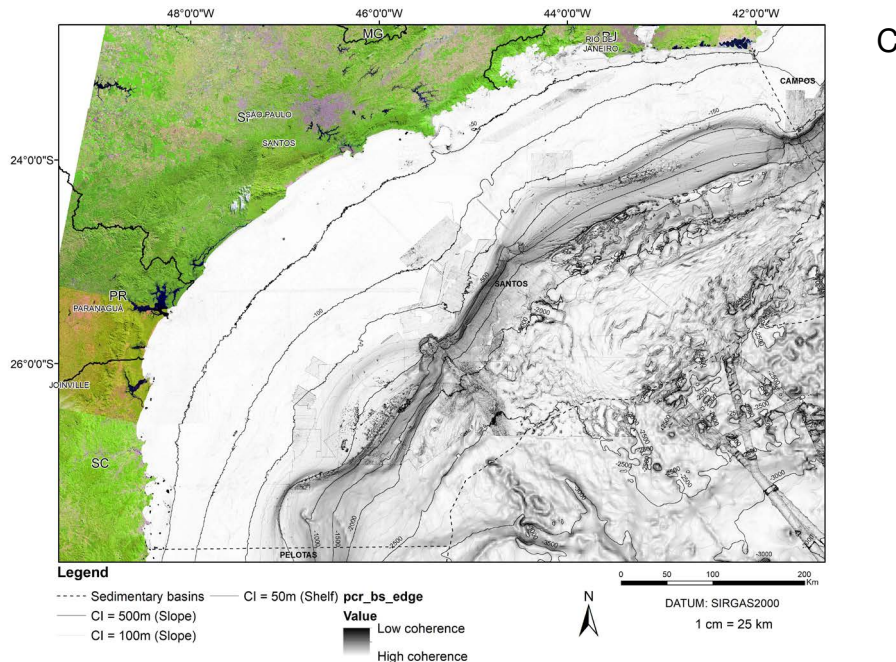


**Figure 4.** (A) Bathymetry map of the Santos Basin, (B) gradient map of the Santos Basin, and (C) coherence (edge) map of the Santos Basin.

## RESULTS

The integrated analysis of bathymetric data, gradient variation, and the 18 profiles crossing the slope and the SPP delimited the boundaries between the continental shelf, continental slope, and the São Paulo Plateau and divided the slope into four geomorphological domains. Moreover, by evaluating the coherence attributes (edge map) and seismic facies in the subsurface, we interpreted the kinds of medium- and small-scale seafloor geomorphic features with resolution in the derivative grids and grouped them according to their similarities.

Most of the continental slope and the São Paulo Plateau are covered by a centimetric pelagic/hemipelagic drape of the Holocene (with a 31 cm average thickness) with a predominance of ooze, marls, and mud. Siliciclastic and carbonate sandy sediments occur in the upper and middle slopes, which also contain bioherms.

The integration between the seismic attributes in the acoustic records and the sedimentological and biostratigraphic data from the bottom sediment samples of the Santos basin enabled the interpretation that the local deep-water seafloor morphology is a relict and formed up to the Pleistocene. The seafloor horizon represents

a sedimentary layer with a thickness ranging from 6 to 10 m, of which only 31 cm, on average, represent the Holocene sedimentary record.

## REGIONAL PHYSIOGRAPHY

The Santos Basin comprises three main physiographic provinces: its continental shelf, continental slope, and the São Paulo Plateau (Figure 5), whose limits are inferred based on gradient average and breaks in a regional scale analysis. The shelf break and slope toe lie at water depths of about 200 and 2000 m, respectively (Figure 6). Most of the basin, about 76% of its total area, shows a declivity of less than one degree due to a wide shelf (76-197 km wide, 815 km long), upper slope terraces, and the massive gently dipping São Paulo Plateau beyond the slope toe. Only 8.8% of the total area shows declivities from two to eight degrees and 0.6%, declivities greater than eight degrees. These areas correspond to a relatively narrow slope (65 km wide in its central part and 115-126 km wide in its southern and northern sectors, respectively), flanks of submarine depressions (valleys and pockmarks), and steeper slopes of salt-related topographic highs in the lower slope and the São Paulo Plateau.

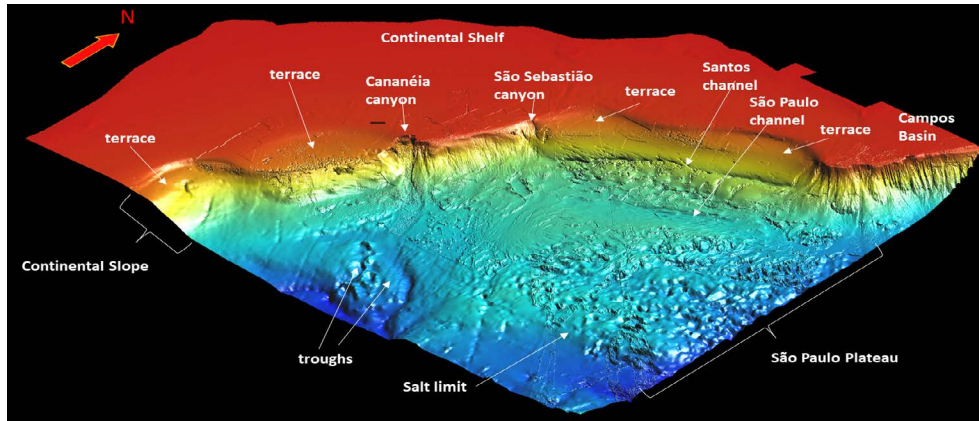


**Figure 5.** Digital elevation model of the Santos Basin seafloor with vertical exaggeration showing the physiographic provinces and medium-scale morphological features.

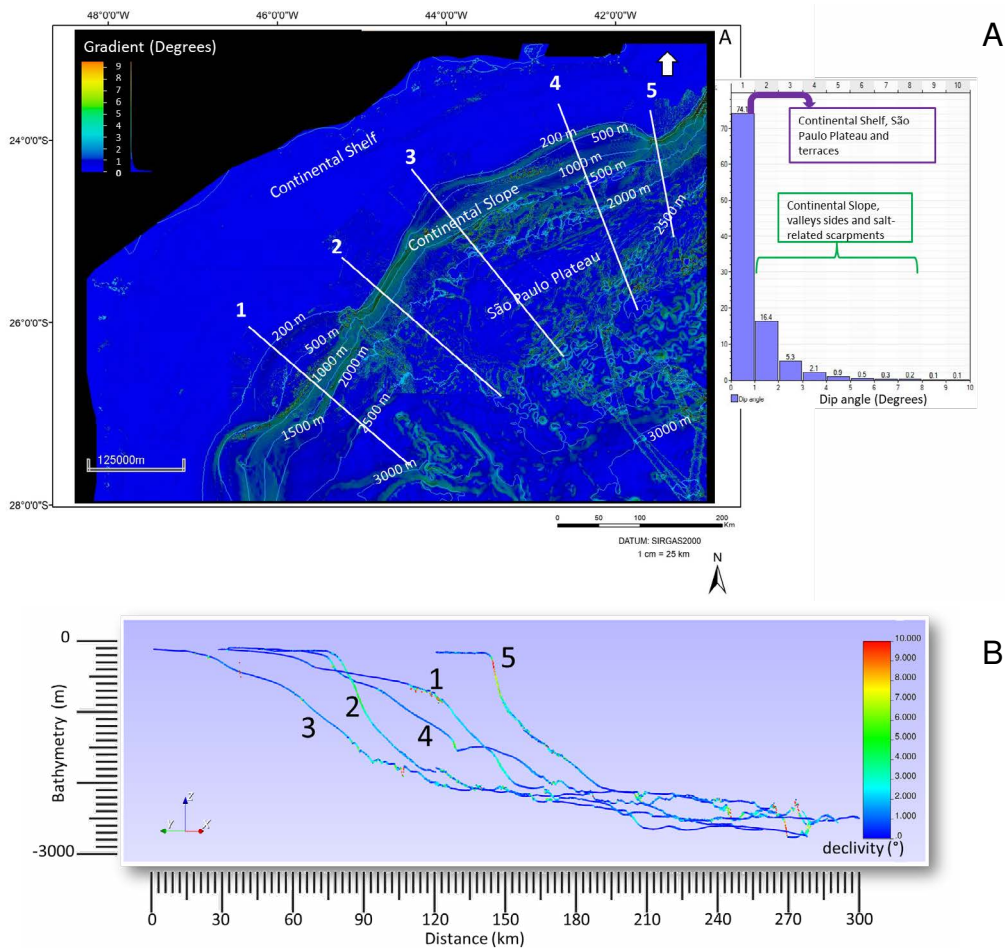


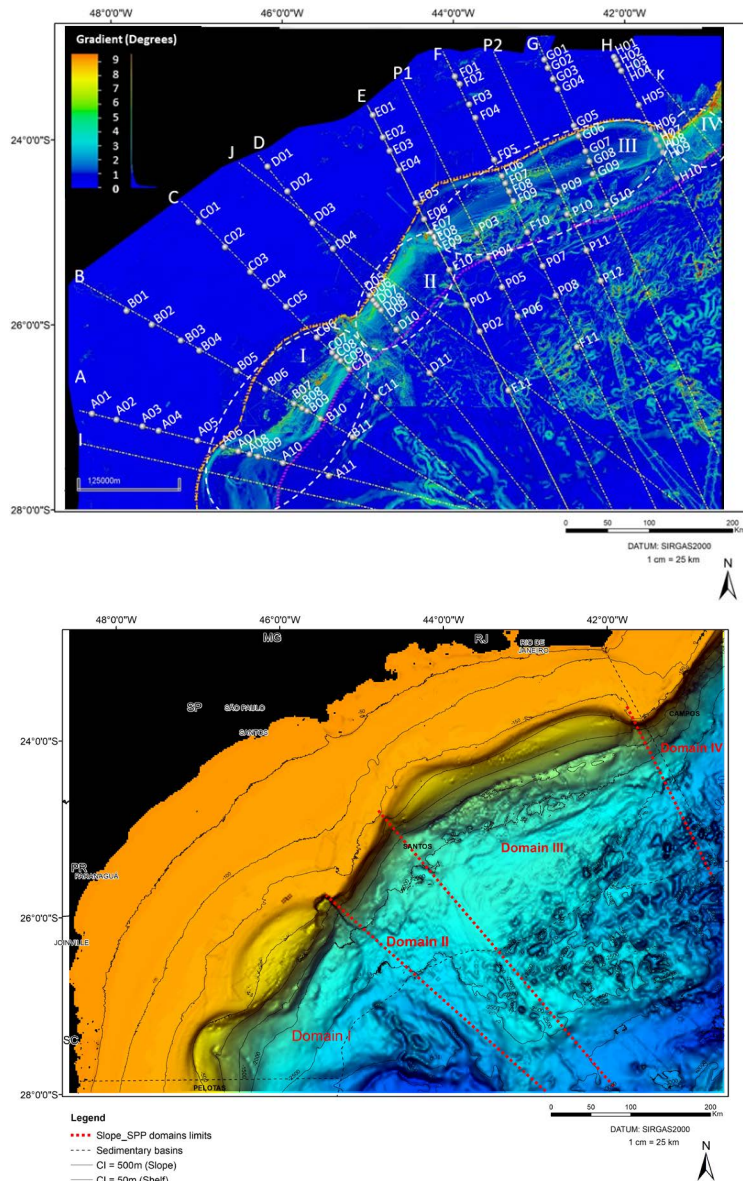
**Figure 6.** (A) Gradient map of the Santos Basin highlighting its main physiographic provinces and histogram of the gradient values, (B) Five profiles shaded according to their average gradient showing the differences in each sector of the continental slope. Profile 1 (southwestern sector) shows a large terrace that gives it a convex shape (Figure 8). The highest gradient average occurs in the upper portion of the middle slope and in the lower slope. Profile 2 (central sector) shows the highest gradient average in the upper-middle slope (Exponential profile; Figure 9). Profiles 3 and 4 (northeastern sector) show narrower terraces and the highest gradient average in the upper (4) and lower slopes (3 and 4), giving them convex and mixed shapes, respectively (Figure 10). Profile 5 shows the highest gradient average in the upper slope, which gives it an exponential shape (Figure 11).

The continental slope of the Santos Basin spans over 780 km in a NE-SW shoreline-parallel trend, changing from N45E to N60E in the northern part. The Santos continental slope outline lies subparallel to the Aptian Hinge line and its northern slope is parallel to the Cabo Frio Fault trace.

### GEOMORPHOLOGICAL DOMAINS

This study subdivided the slope and its adjacent SPP into four geomorphological domains

(I- southwestern, II- central, III- northeastern, and IV- far northeastern) based on their direction, profile, average gradient, shelf break isobath, and the distribution of the medium-small scale geomorphic features, which this study evaluated based on regional profiles integrated with bathymetry and gradient maps (Figures 6 and 7). The SPP shows considerable geomorphological variations related to the occurrence or absence of evaporites.



A

B

**Figure 7.** (A) Gradient map of the Santos Basin with regional profiles (dashed white lines) across multiple physiographic provinces and domains (I, II, III, and IV). White dots with white labels refer to sediment sample sites of the PCR-BS. Profiles A, B, C, D, E, F, G, H, P1, and P2 contain the sample sites. The dashed orange line represents the shelf break and the dotted pink line, the slope-SPP boundary; (B) Shaded bathymetric map showing the geomorphological domains.

Table 1 summarizes the main characteristics of the local geomorphological domains and points out their differences. The Discussion

section addresses the main geological processes that induced the alongslope and downslope geomorphological variations.

**Table 1.** Main characteristics of the geomorphological domains separated by bathymetric range.

| Geomorphological Domains | I   | I               | II   | II                   | III   | IV   |
|--------------------------|---|-----------------|--|----------------------|---|--|
| Regional Profile         | Convex/linear   |                 | Exponential  |                      | Mixed (Linear, slightly convex -concave)  | Exponential  |
| Orientation              | N45W  |                 | N45W   |                      | N60W  | N60W   |
| Upper Slope              | Large terraces (26-57 km wide) with pockmark fields   |                 | Steep Upper slope Scars head, ravines, MTD*                                  |                      | Narrower terraces (20-36 km wide) with pockmark fields, unit pockmarks  | Steep Upper slope. Scars head, MTD*  |
| Middle Slope             | Scars and MTD*  | Canyon Cananéia | Ravines, scars, and MTD*   | Canyon São Sebastião | Countourite Drift (Santos Drift), pockmarks, bioherms   | Scars and MTC**  |
| Lower Slope              | Small scars and MTD*  |                 | Salt minibasins, ridges, and crestal grabens without a preferred orientation |                      | Santos Drift (Santos Channel); Salt minibasin, NE-SW crests, and crestal grabens  | MTC**  |
| SPP                      | Submarine valleys connected updip and downdip to the Canyon Cananéia and to a depocenter, respectively. Absence of evaporites |                 | Southward-dipping seafloor, transition between salt and unsalted region      |                      | São Paulo Drift (SPD), São Paulo Channel, Salt minibasin, crests, and crestal grabens, salt related features resembling an egg carton | MTC**, Salt minibasin, crests, and crestal grabens, salt related features resembling an egg carton |

\*MTD- mass-transport deposits; \*\*MTC- mass-transport complexes

The southwestern domain (I) contains two upper slope terraces at water depths from 240 to 700-800 m, defining two embayments, 26-57 km wide, convex/linear profile, and an average declivity of two degrees (Figure 8). The central domain (II) shows the same orientation, lies at N45 W, and has an exponential profile, an average declivity of three degrees, and a straight shelf break at a 200 m water depth (Figure 9). A mature conduit (Cananéia canyon) generated by a vast gravity-driven depositional process marks the limit between these two domains.

The upper-middle slope of Domain II mostly consists of scars, ravines, and two huge canyons at its boundaries, whereas the lower slope and adjacent SPP show a salt minibasin, crest, and crestal grabens with different arrangements from their northern neighbors.

The boundary between the central and northeastern domains is marked by a smaller

canyon, the São Sebastião canyon. The northeastern domain (III) shows a N60 W direction, upper slope terraces at a water depth between 240 m and 700 m, shelf break at the 200 m isobath (which draws two embayments, 20-36 km wide), linear/exponential profile, and an average declivity below 1.5 degrees (Figure 10). The upper and middle slopes in this domain show a smooth seafloor relief at a water depth of up to 1500 m, unlike the lower slope, which shows relief variations related to halokinesis (salt minibasins and ridges).

The far northeastern domain (IV), situated at the boundary with the Campos Basin, presents a steeper upper slope (5 degrees, on average) and a middle/lower slope with an average declivity of two degrees, exponential profile and shelf break at 200 m (Figure 11). Its toe slope lies more deeply (2000 m water depth) and comprises a mass-transport complex apron.

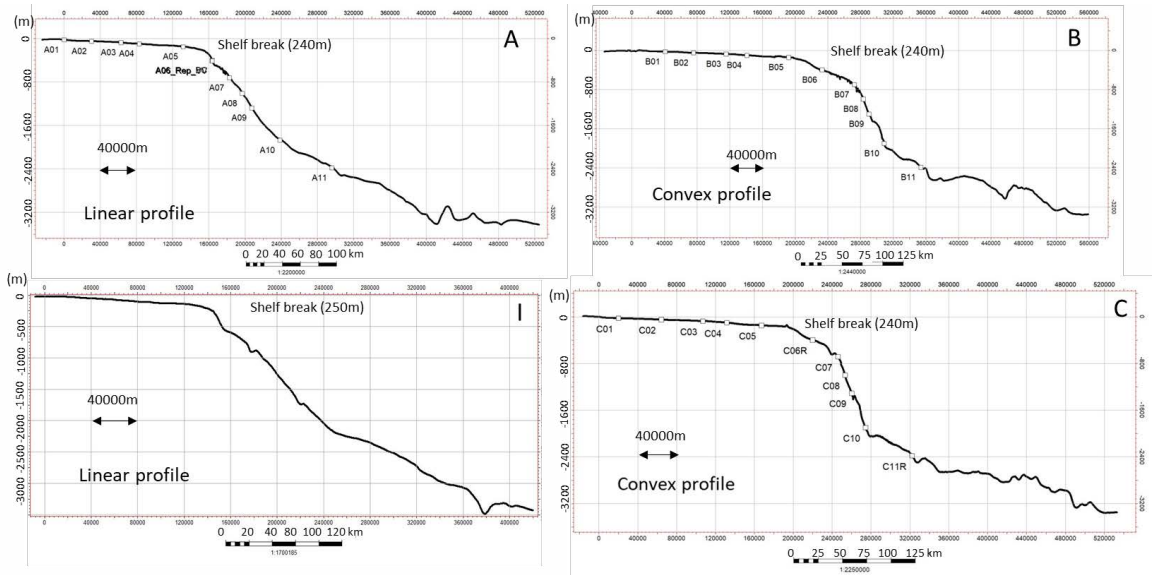


**Figure 8.** Domain I regional profiles showing the shelf break, the upper slope terraces (B and C profiles) that give a convex profile to the slope, and the linear profiles of the basin southernmost slope (A and I). Unlike the contiguous slope northward, the southernmost slope shows the steepest slope after the shelf break, followed by a narrow terrace. Vertical exaggeration 60×.

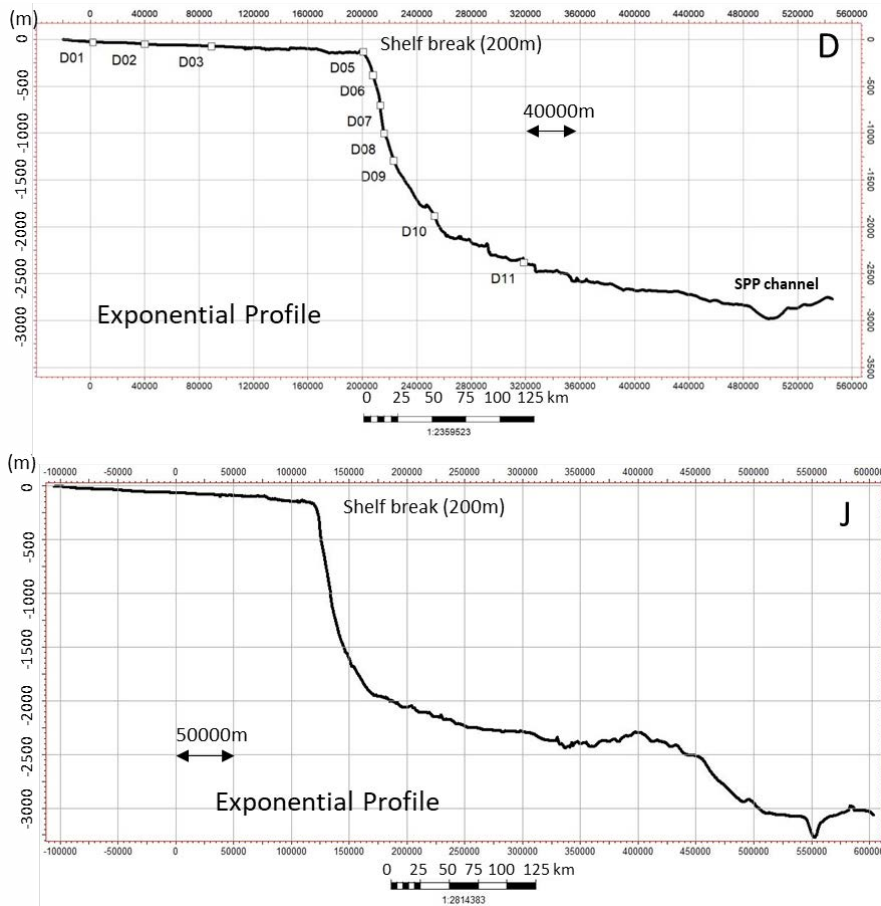


**Figure 9.** Regional profiles of Domain II (D and J) showing a steep upper slope that gives its profile an exponential/concave character. Vertical exaggeration of 60×.

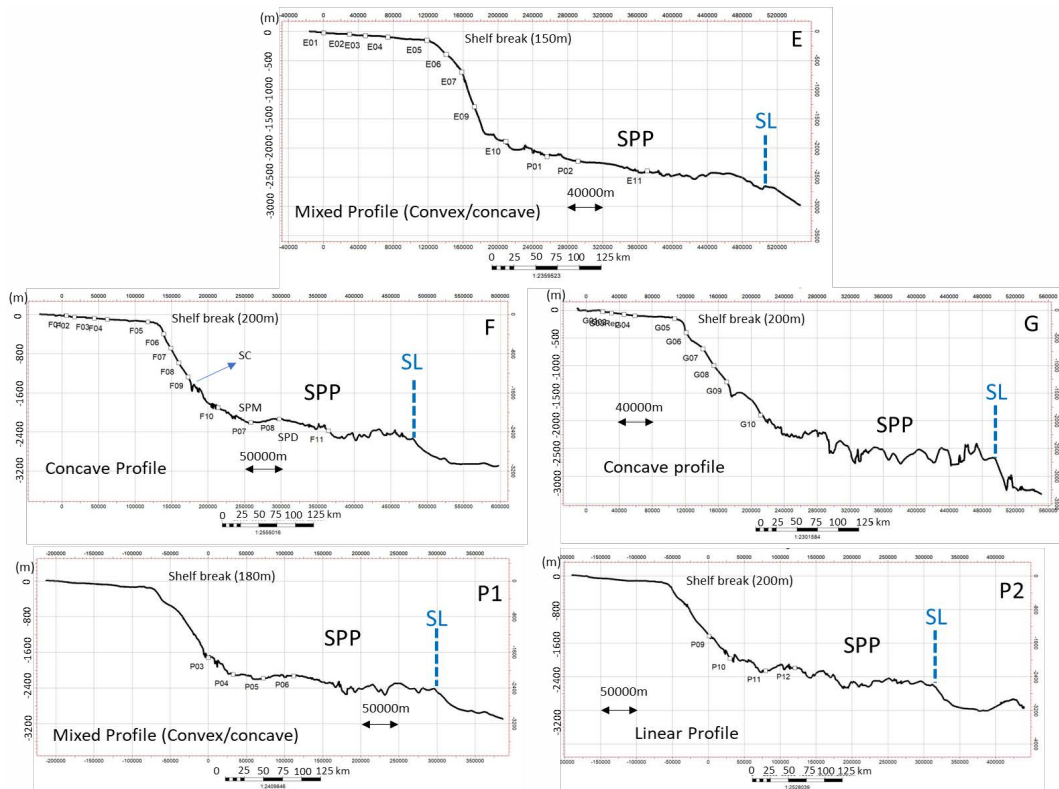


**Figure 10.** Regional profiles of Domain III (E, P1, F, P2, and G) mainly showing mixed (slightly convex/concave) and linear profiles. These regional profiles reach the SPP external scarp. All profiles show the rough relief of the SPP, except profile E, which reaches the deeper portion of domain II, which is less deformed. In contrast, profile G includes the most deformed salt domain. 60× vertical exaggeration. SL-salt limit, SPD-São Paulo drift, SPM-São Paulo moat, SC- Santos channel.

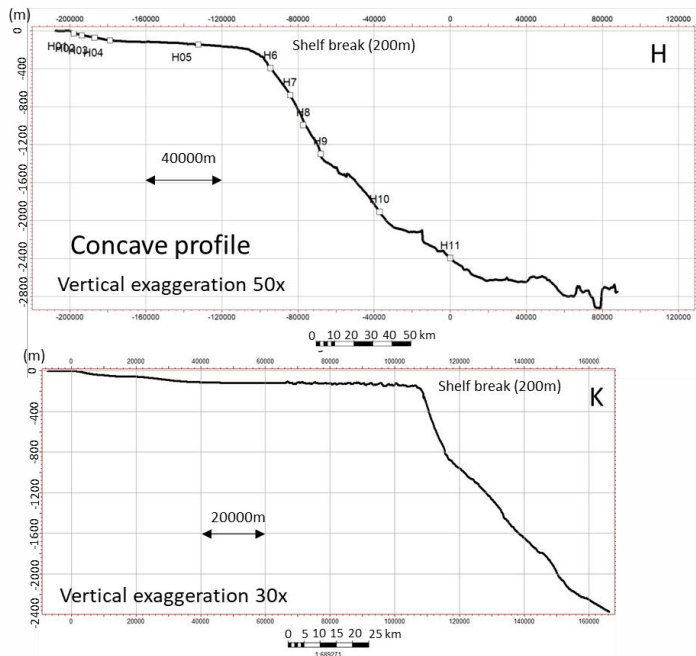


**Figure 11.** Profile K belongs to domain IV, and profile H (concave) crosses the boundary between domains III and IV. Profile K shows a steeper upper slope, whose highest gradient average gives it an exponential shape in the regional view (see Figure 6).

Salt deeply affects the SPP seafloor geomorphology of domains II and III, unlike domain I, which includes southeast flowing channels and no salt at the SPP. In this domain, the eastern boundary of evaporites roughly coincides with the slope toe.

Some authors correlate the large-scale physiography and even medium-scale seafloor features with the interaction between bottom currents and the seabed (Duarte and Viana, 2007; Schattner et al., 2016, 2018; Mahiques et al., 2017, 2022; Ramos et al., 2019). According to Duarte and Viana (2007), the large-scale physiographic sinusoidal configuration of the shelf-slope transition could be related to the meandering and gyre detachment of the slope by the Western Boundary Brazil Current that penetrates the onshelf.

Silveira et al. (2022) described the oceanic circulation over the continental slope and SPP

during the winter of 2019. Circulation is dominated by the southward-flowing Brazil Current, the Intermediate Western Boundary Current (IWBC) and their meanders, and the remotely generated anticyclones and cyclones. The Brazil Current extends from the surface to 400-550 m, and the IWBC acts from a water depth of 550-1300 m, with a core at about 900 m. The IWBC is formed in the southern Santos Basin from a bifurcation of the South Equatorial Current (SEC), which is impacted by a cyclonic loop provoked by the SPP (see Figure 1 from Silveira et al., 2022).

### MEDIUM- TO SMALL-SCALE SEAFLOOR GEOMORPHIC FEATURES

Table 2 summarizes and Figure 12 compiles the main medium- and small-scale geomorphological features of the Santos Basin seafloor.

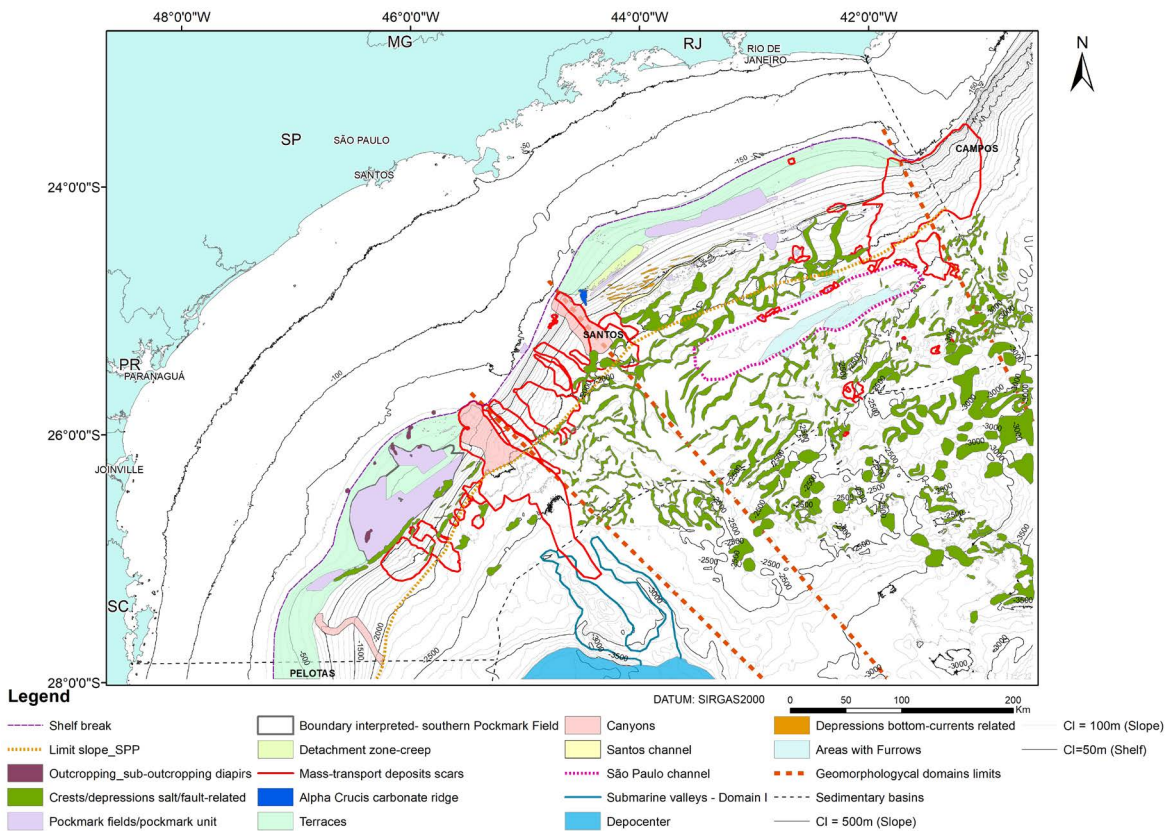


**Figure 12.** Geomorphological map showing the main geomorphic features mapped in the slope and SPP of the Santos Basin.

**Table 2.** Main morphological features in the deep waters of the Santos Basin and related geological/biological events.

| Morphological features and associated geological / biological events           |  |
|--|--|
| Morphological Features   | Geological Events  |
| Small and medium scale seafloor roughness                                      | Gravity-driven processes (mass-transport deposits buried or surficial) |
| Scars  | Gravity-driven processes (slope failure and mass transport)            |
| Undulated seafloor (large wavelength - 1 to 10s of km)                         | Contourite drifts  |
| Undulated seafloor - sediment waves (wavelength smaller than 1 km)             | Gravity-driven processes (turbidity currents) or bottom currents       |
| Valleys (canyons, channels, ravines, gullies, moats)                           | Gravity-driven processes or bottom currents                            |
| Salt-related topography (salt minibasin, diapirs, and walls, crestral grabens) | Halokinesis/Halotectonics  |
| Pockmarks  | Fluid migration/Seepage/Fluid expulsion on the seafloor                |
| Erosive terraces   | Erosion by bottom currents or gravitational flows                      |
| Depressions, furrows   | Erosion by bottom currents   |
| Carbonate mounds, pinnacles, ridges  | Bioherms   |

## POCKMARKS

This study interpreted several circular to elliptical depressions in the upper slope of the southern and northeastern domains as pockmarks, which record fluid escape on the seabed. It also observed some giant pockmarks in the lower slope of the northeastern domain.

Pockmarks occur as a single feature or are organized in a train array. They sometimes coalesce to form an elongated depression. Some are associated with faults at depth. Many giant pockmarks contain minor pockmarks. Carbonate mounds and pinnacles (bioherms) also occur inside many pockmarks, locally showing a needle-like relief.

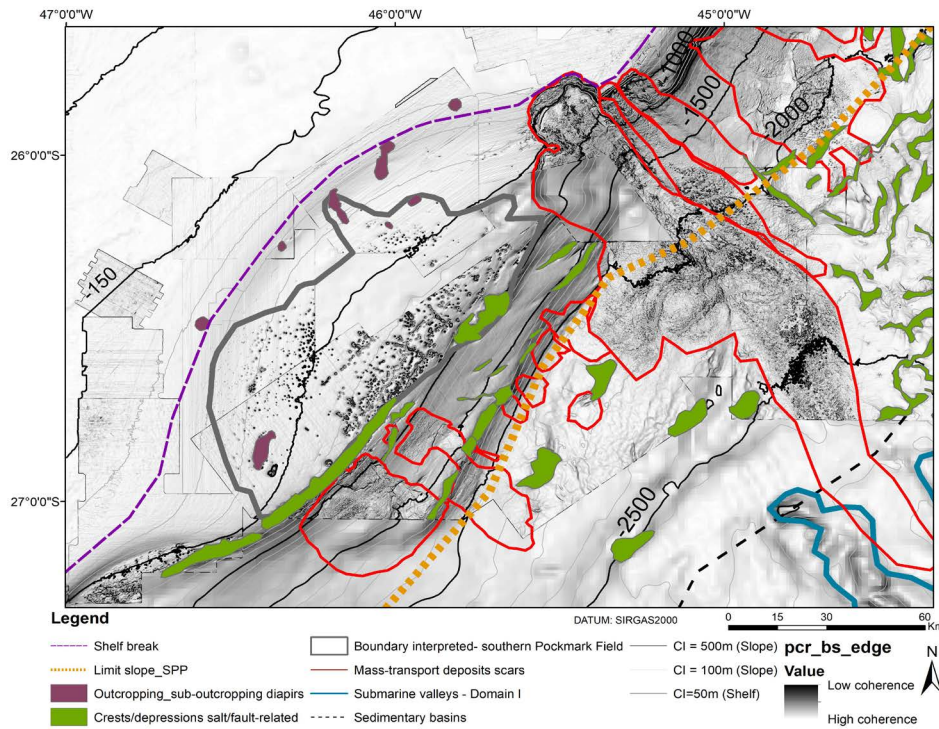
The southwestern domain (Domain I) shows a larger, 125 km long pockmark field at a water depth from 300 to 1100 m with a denser occurrence near the terrace eastern boundary that becomes sparse to the west, south, and northeast (Figure 13). Some of these pockmarks locally occur in the middle slope, up to the 1100 m isobath. The far southwestern terrace was not covered by 3-D seismic or high-frequency surveys that would highlight these kinds of features. Pockmark diameters vary from 200 to 1500 m, most often from 300 and 500 m. Some pockmarks in this domain are associated with exhumated diapir flanks or salt-related crestral graben faults. Downslope of the pockmark field,

large scars occur due to gravity-driven processes, mainly slumps and debris flows.

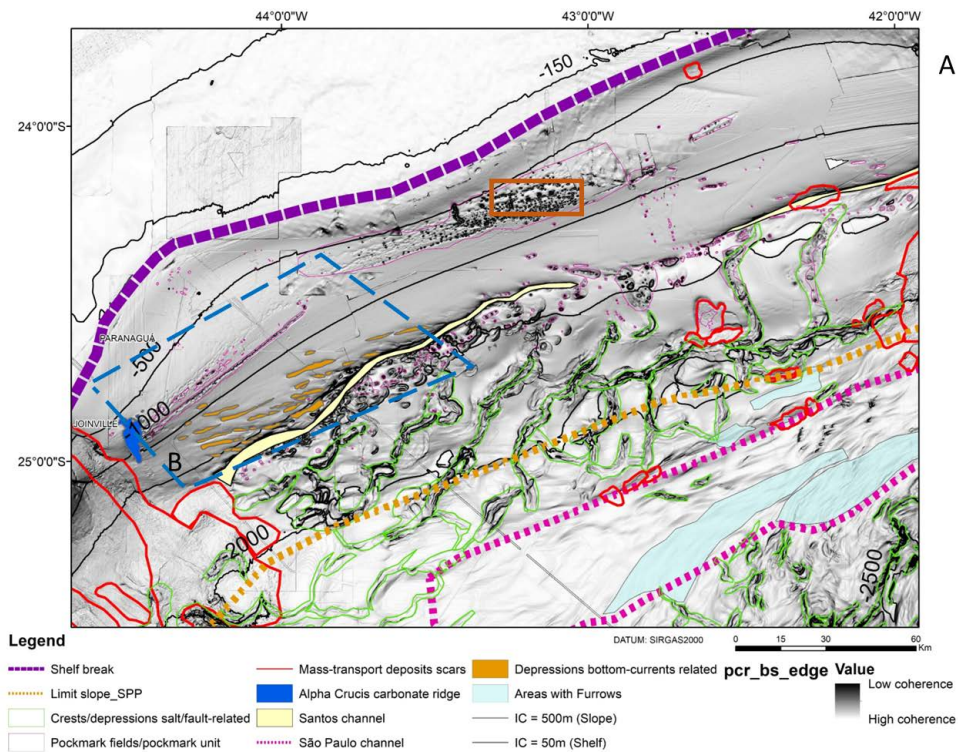
Mahiques et al. (2017) described part of this large pockmark field at 300-700 m water depths in the southern Santos Basin using high-resolution multibeam bathymetric data. They found 984 pockmarks in linear, network, concentric, and radial patterns and numerous buried and exposed salt-diapirs with crestral faults based on 2-D multichannel seismic data.

Schattner et al. (2016) correlated the pockmark geometry of the upper slope of domain I with the SW-trending Brazil Current flowing down to a water depth of 500 m and the NE-trending IWBC flowing below a water depth of 500 m. These currents modify the pockmark original circular and conic profile to an elliptical shape and asymmetrical profile.

Pockmark fields also occur in different ranges in the northeastern domain (Domain III). The shallow ones lie at a water depth of about 200 to 300 m and are sparsely distributed. A denser pockmark field occurs at a water depth from 500 to 900 m, in which pockmark diameters vary from 150 to 2000 m. Along the 800 m isobath, a straight 50 m wide, 60 km long, and with a 45 m-8 m relief NE-SW step depression occurs southward with aligned pockmarks. This depression contains bioherms forming needle-like pinnacles and some discrete pockmarks situated upward. Carvalho et al. (2022) found cold-water corals at this site (Figures 14, 15, and 16).



**Figure 13.** Shaded bathymetry map of the southwestern domain (Domain I) showing a larger pockmark field between 300 m and 1100 m water depth, 125 km long, with a denser occurrence near the terrace eastern boundary that becomes sparse in the west, south and northeast directions. The pockmark diameters vary from 200 m to 1500 m, with most frequent diameters between 300 m and 500 m.



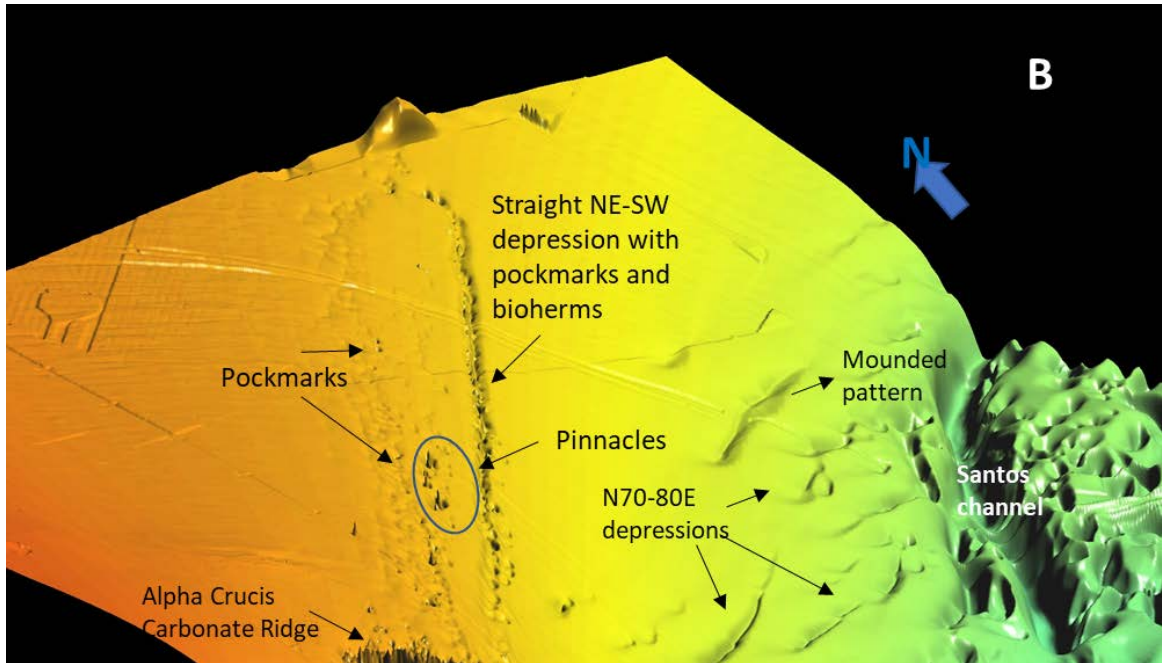


**Figure 14.** (A) Shaded bathymetric map showing the main pockmark fields of the northern domain (III). The shallower field lies at about 200 to 300 m water depth, in which the pockmarks are sparsely distributed. The denser pockmark field occurs in the 500-900 m isobaths. The southwestern portion of Domain III contain the Alpha Crucis Carbonate Ridge and a NE-SW depression with pockmarks and bioherms. From the 1400 to 1800 m isobaths, pockmarks are sparsely distributed within and outside elongated depressions (crestal grabens). Most are concentrated along the Santos channel. (B) Digital elevation model comprising the blue polygon area (see location in map A) with vertical exaggeration to show the straight NE-SW stepped depression with aligned pockmarks and bioherms that contain cold-water corals and narrow N70-80E depressions that could be related to IWBC reworking and fluid escape. Figure 15 represents a magnified view of the area delimited by the orange polygon.

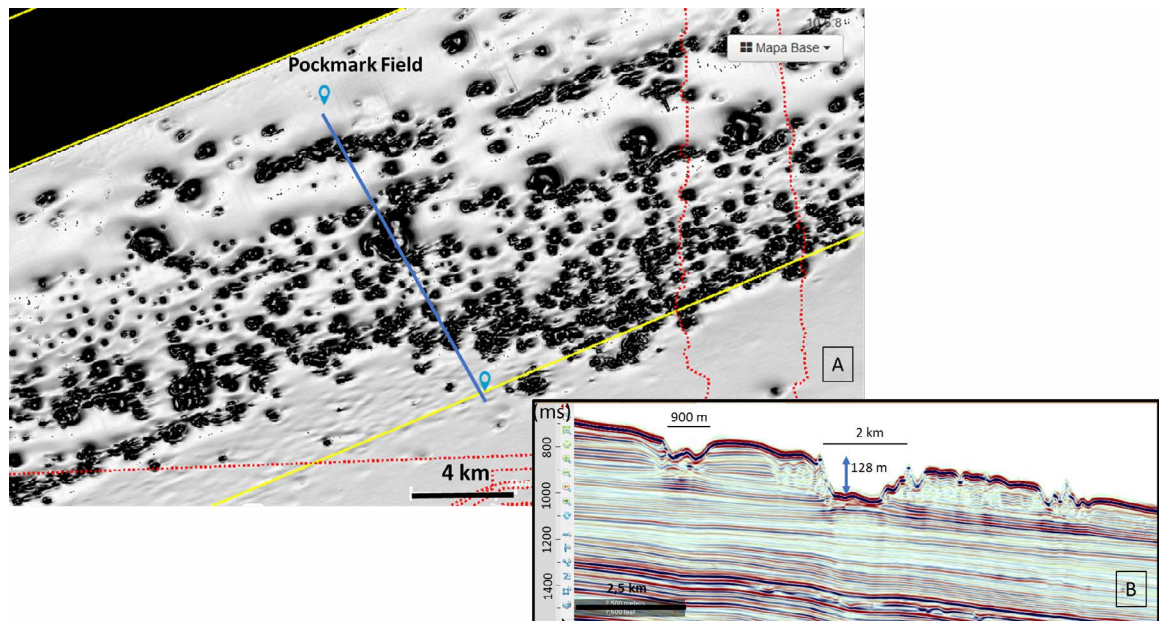


**Figure 15.** (A) Coherence (edge) map showing the northern upper slope pockmark field, mostly aligned in a NE-SW direction. (B) Seismic profile (vertical scale in ms-millisecond), with vertical exaggeration, crossing one of the largest pockmarks of the field, which has a 2 km diameter and a 128 m relief height. Location in Figure 14. (TWT: two-way travel time on the y axis).

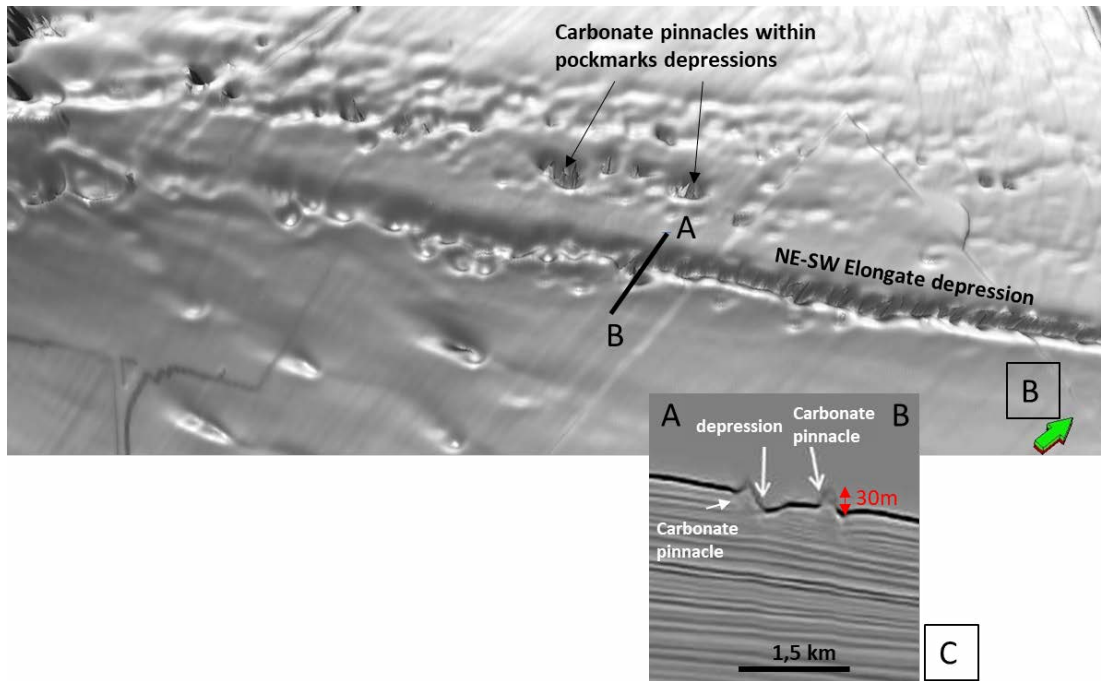
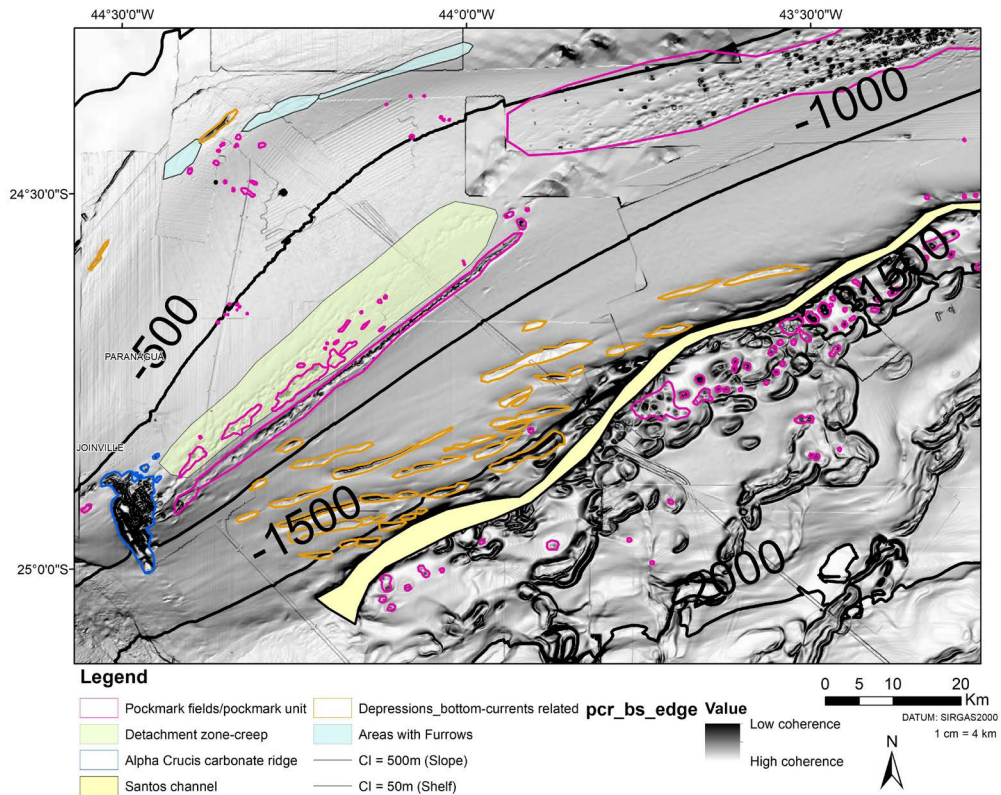


**Figure 16.** (A) Coherence (edge) map showing the main geomorphological features of the northern domain (III), (B) Digital elevation model with vertical exaggeration showing the straight NE-SW depression associated with pockmarks and carbonate pinnacles (bioherms) in the edge map (pink narrow elongated polygon), and circular pockmarks up dip with associated pinnacle, and (C) Seismic profile crossing the linear depression with needle-shaped pinnacles. Southeast of the NE-SW depression, orange polygons highlight the N70-80E bottom current-related depressions.

The water depth from below 1400 up to 1800 m contain sparsely distributed pockmarks within and outside elongated depressions (crestal grabens), with diameters up to 1500 m. Most are concentrated along the Santos channel. Some major depressions contain small pockmarks.

## CANYONS

Duarte and Viana (2007) first described and named the only two canyons that cut the continental slope of the Santos Basin: the Cananéia and São Sebastião canyons. According to the authors, the Cananéia canyon coincides with a crustal lineament, the Capricórnio lineament, defined by Bueno et al. (2004).

The Cananéia canyon is a massive (85 km long), mature conduit that probably stems from successive retrogressive collapses (slumps) and reaches the 200 m isobaths. It has a 23 km wide and 370 m high large stepped head. The canyon scar is filled by mass-transport deposits with runout distances longer than 140 km and a flow to the NW-SE SPP channels region. Although these deposits are buried, they affect seafloor relief roughness (Figures 5 and 12).

The São Sebastião canyon shows a smooth talweg relief with a smaller (17 km wide) head cut by gullies, converging to the SPP area of salt-related highs and minibasins. The canyon head reaches the 300 m isobath.

## SALT MINIBASIN-RIDGE-CRESTAL GRABENS

Salt minibasins consist of smooth-relief depressions surrounded by salt-related highs, which, in turn, are associated with salt walls at depth. Crestal elongated grabens are depressions formed by the collapse of the faulted wall crest. Most geologic faults that reach the seafloor or lie near the surface are associated with salt crests and crestal grabens.

In the lower slope (below the 1500 m water depth) and the SPP of the northeastern domain (III), halokinesis/halotectonics affected the seafloor relief, resulting in NE-SW narrow crests and crestal grabens that extend for tens of kilometers and are flanked by a minibasin, whose genesis is linked to normal listric faults at depth. These minibasins span from 250 to 720 km<sup>2</sup>. Salt movements have more intensely affected the SPP eastern than the lower slope, probably because its diapirs and walls experienced a more significant lift in response to the presence of the External High (Figures 12 and 14).

The lower slope of the central domain (II) has the same geomorphic features (salt minibasins, crests, and crestal grabens) but with a smaller relief and area and WNW-ESE and NNE-SSW crest orientations (Figure 17). These minibasins range from 45 to 240 km<sup>2</sup>. The SPP of the central domain contains the evaporite limit and a southward-dipping seafloor.

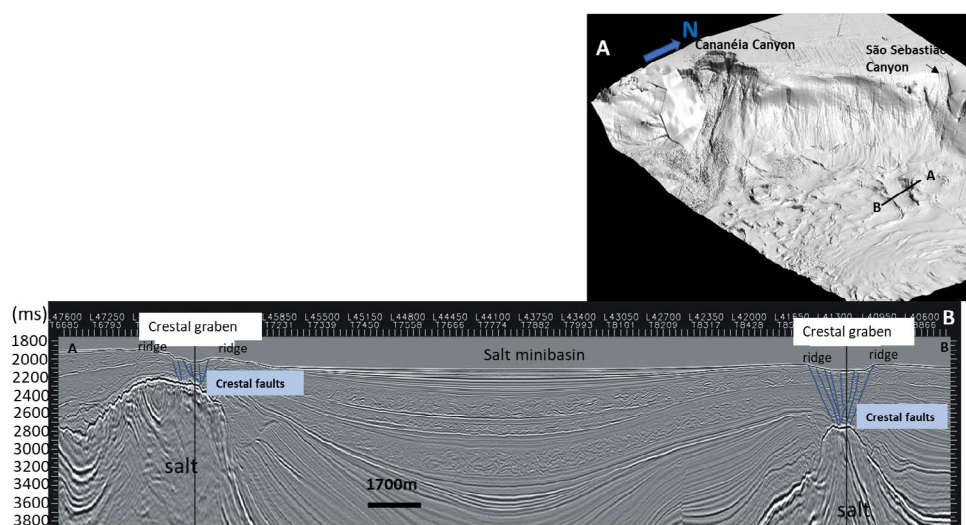


**Figure 17.** (A) Digital elevation model with vertical exaggeration to highlight the main geomorphological features of the central domain (II) and (B) the seismic profile (vertical scale is TWT: two-way travel time in ms) crossing an SPP NW-SE salt minibasin-ridge-crestal graben set. The salt minibasin has a smooth seafloor relief and is filled by parallel strata that onlap salt-related highs.

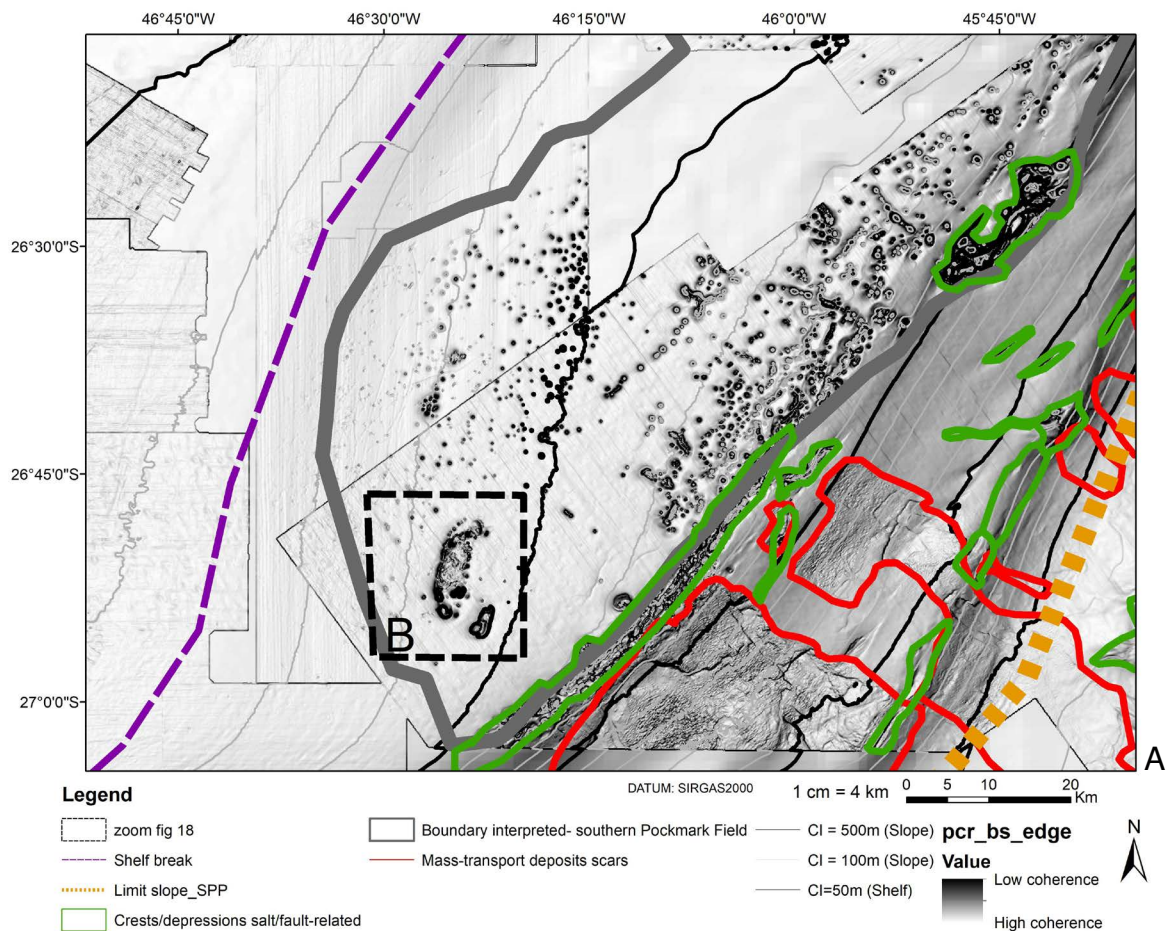
The diapirs in the southwestern domain (I) mostly lie in the continental slope. The upper slope contains shallow and exhumed diapirs from 240 to 800 m water depths, one of which is surrounded by fault-related elongated depressions and pockmarks that were reworked by the ocean bottom current. The middle slope has innumerable well-developed NE-SW depressions below the 800 m water depth (2-7 km wide, 7-90 km long) that are related to crestal diapir faults reaching the seafloor. These depressions may be associated with fluid seepages and probably were deepened and enlarged by the IWBC. Some crests that delimit such depressions may be populated by bioherms. Some major depressions also show rough seafloor relief (probably associated with surficial slides).

On the lower slope, shallow diapirs have induced a slightly topographic high, running from

NE to SW, whose activity probably triggered many smaller slope failures in which scar heads reached the high eastern flank along the 1500 m isobath (Figures 12 and 13).

### PIERCING AND EXHUMATED SALT DIAPIRS

Some outcropping and suboutcropping diapirs occur on the upper slope of the southwestern domain (I), one of which is a prominent exhumed diapir surrounded by an elongated depression and pockmarks — which are highlighted in the edge map (Figure 18). Schattern et al. (2018) studied the pre-exhumation piercing phases of this diapir and its interaction with ocean bottom currents. They stated that these currents reworked the crestal faults of the shallow diapir phase to form this elongated depression.



[continued]

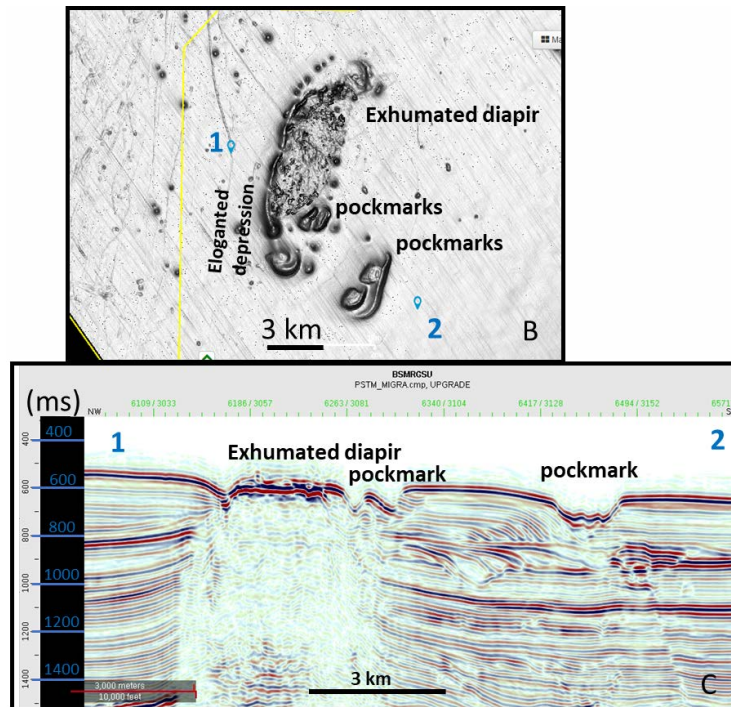


**Figure 18.** (A) Edge map showing the main features of the southern domain: an extensive upper slope pockmark field, exhumed diapir, NE-SW fault-related depression in the middle and lower slope, scars comprising mass-transport deposits, (B) Exhumed diapir and its surrounded depressions in detail, and (C) Seismic profile crossing the diapir and pockmarks (vertical scale in ms).

### SCARS AND MASS-TRANSPORT DEPOSITS

Innumerable slope-failure scars and mass-transport deposits occur in the southern, central, and uppermost northeast domains of the Santos Basin slope. Scars occur more frequently in the southern, central, and far northeastern domains and have greater size than the scars in the northeastern domains, where they are rare and smaller and lie mostly near/below the limit of the 3-D seismic data resolution (Figure 19). Domain I shows scars areas varying from 46 to 5250 km<sup>2</sup> and averaging 930 km<sup>2</sup>. The scars in domains II and III average 800 km<sup>2</sup> and 46 km<sup>2</sup>, respectively. Domain IV shows the largest scar of the basin (spanning 6700 km<sup>2</sup>), comprising many smaller scars to form a huge mass-transport complexes that exceeds the limits of domain IV toward domain III to the south, and the Campos Basin to the north.

The southern upper slope, upstream of the mass-transport deposit scars, contains an extensive pockmark field, with some pockmarks associated with faults at depth or diapir flanks. Massive square head scars occur over the middle slope, some of which reach the terrace boundary.

Most scars contain an associated rough relief that is related to mass-transport deposits. Some mass transports are surficial slides with shallow detachment surfaces situated about 20 m below the seafloor (Figure 20).

In the central domain, scars with minor heights smooth the relief contrast, and mass-transport deposits are concentrated in the lower slope. The far northeastern domain has the steepest slope and shows extensive mass-transport complexes that form a slope-apron in the lower slope and SPP.

A series of crescent-shaped depressions below the upper-middle slope boundary occur in the northeastern domain, coinciding with a slight increase in the gradient. This study interpreted these morphological features as scars associated with a slow displacement of the seafloor along a slip surface (creep processes, Figure 16).

Piston cores and high-frequency seismic data show that most mass-transport deposits are older than 10 ky (dating to the Pleistocene or before). Although most mass-transport deposits are buried, their irregular tops are mimicked in the sea bottom relief by pelagic/hemipelagic drapes.

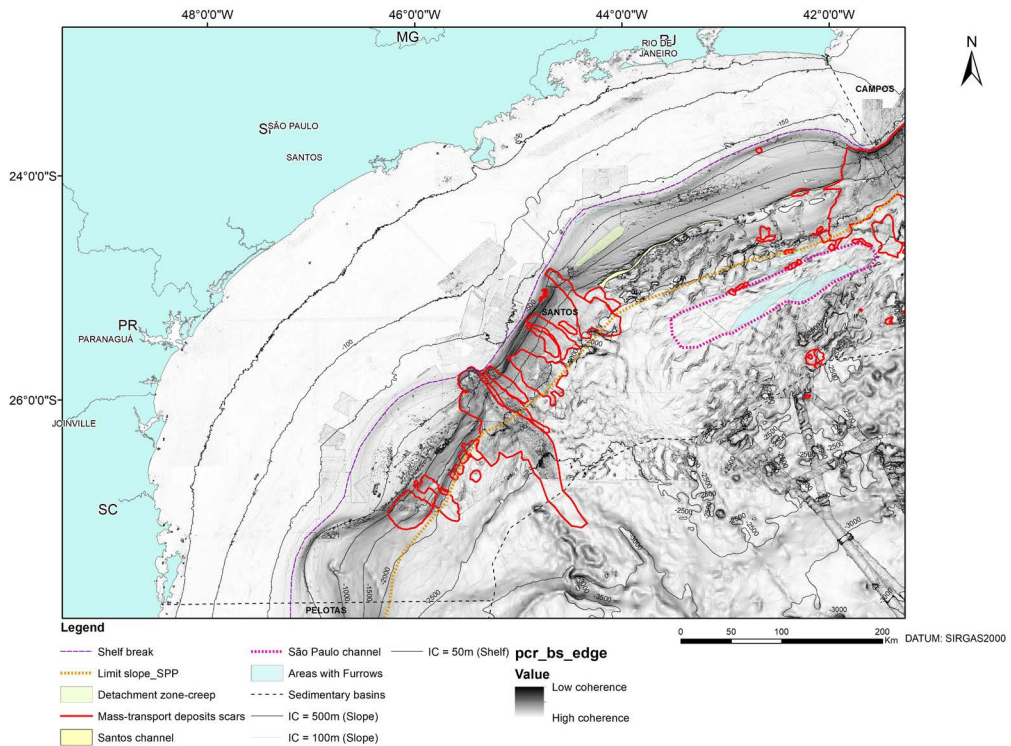


**Figure 19.** Coherence (edge) map highlighting the geomorphological seafloor features (especially mass-transport complexes: scars and deposits, delimited by red polygons) that predominate in the southern, central, and far northern domains (I, II, and IV). The southern domain has small scars aligned with a NE-SW lower slope slight crest that contains its head scars. The small scars mapped in the SPP are usually associated with oversteepened salt-related topographic highs.

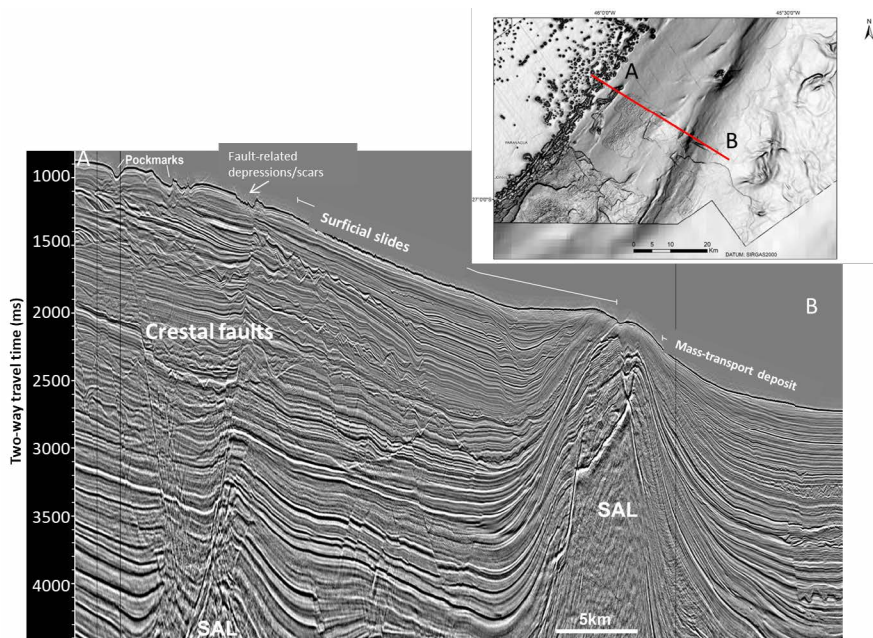


**Figure 20.** Seismic profile (vertical scale in milliseconds) of the southwestern slope showing the pockmarks and elongated depressions associated with salt crestal faults that reach the seafloor, downdip occurrence of a square head scar (see location map) comprising an undulate seafloor associated with a surficial slide, and the eastward occurrence of a salt-related topographic high with a steepened eastern flank that experienced failure and mass transport processes.

## CONTOURITE DRIFTS AND OTHER BOTTOM CURRENT-RELATED FEATURES

Duarte and Viana (2007) recognized a vast drift system (300 km long, 200 km wide, and 1 km thick) in the northern Santos Basin (Domain III), which developed from the Late Palaeogene to the Recent, named the Santos Drift System (SDS - Figure 21). According to the authors, the SDS spans from a depth of 200 m to more than 3000 m and can be subdivided into two main contourite drifts: the Santos Drift (SD) and the São Paulo

Drift (SPD). The SD lies at 200-2000 m water depths and consists of a slope-plastered drift that is genetically related to a narrow, slope-parallel channel named the Santos Channel, developed from the Oligocene to the present. The SPD is developed in association with a moat, the São Paulo Channel, which approximately coincides with the gradient break in the passage of the toe slope-SPP. The researchers also recognized furrow-like features in the SPP associated with the SPD.

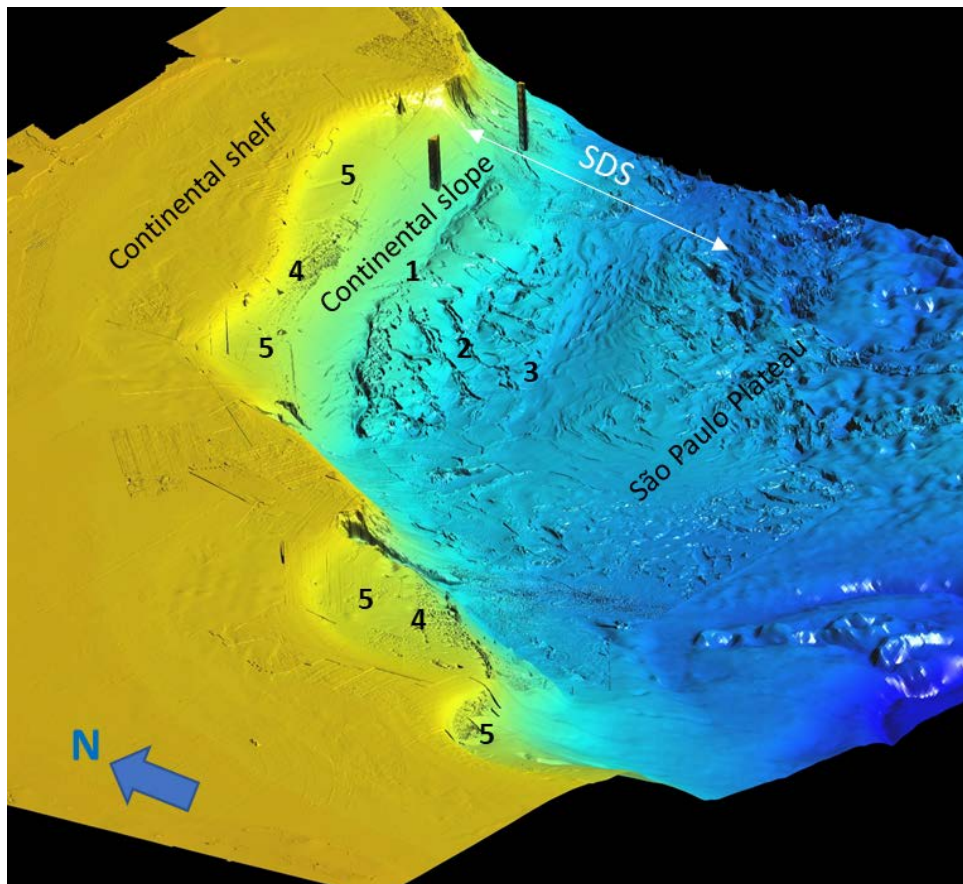


**Figure 21.** Digital elevation model with vertical exaggeration to highlight the Santos Drift System (SDS) and main medium-scale geomorphic features of the upper slope. (1) Santos channel, 2- NE-SW salt minibasin-ridges-crestal graben sets of the northeastern lower slope, 3- São Paulo channel, 4- Pockmarks fields, and 5- Upper slope terraces; SDS- Santos Drift System.

In the northeastern domain, from 900 to 1500 m water depths, narrow NE70-80E depressions occur from two to 20 km long, which could be related to IWBC reworking (Figure 16). Mahiques et al. (2022), from a chirp sub-bottom profile of some depressions in the northern middle slope, described adjacent seafloor mounded patterns related to the IWBC

north-eastwards flow action. The authors also found a depression upward associated with wipeouts at depth, interpreting it as possible fluid escape.

Depressions and furrows aligned to the shelf break also occur on the northeastern upper slope, corroborating other evidence of bottom current action in domain III (Figure 16).

## OTHER SUBMARINE VALLEYS

In addition to these canyons, the slope and plateau contain other types of submarine valleys, such as ravines and deep-water troughs.

Ravines occur in the central and northern slopes. Most ravines in the northeastern domain lie in the upper slope and are partially or totally filled. In the central domain, a parallel-drainage system that runs downward comprises innumerable narrow valleys interpreted as ravines related to sediment transfer by gravitational flows from the outer shelf to the lower slope and the SPP.

The southern plateau shows two NW-SE well-developed valleys from the 2600 m isobath that flow into a depocenter below 3200 m. These 105-165 km long and 12-15 km wide valleys have talweg depths varying from 100 to 300 m and are connected upward to the Cananéia canyon (Figures 5 and 12).

## BIOHERMS

Carvalho et al. (2023) characterized the diversity and distribution of cold-water corals in five sites in the upper/middle slope (200–1000 m depth) of the northeastern domain (III) using multibeam bathymetric data, remotely operated vehicle images, and bottom samples (Figure 17). The coral assemblage structure, abundance, and richness varies among sampled sites and across depths, with increasing coral abundance and richness toward the northern end of the Santos Basin, near Cape Frio, in which the known eddy-induced upwelling phenomenon probably provides higher food availability to the benthos. The main colonial species in the coral mounds refers to *S. variabilis*, which occurs predominantly under the Antarctic Intermediate Water. *Lophelia pertusa* occurs more abundantly in areas bathed by the South Atlantic Central Water.

Sharp and Badalini (2013), based on 3D seismic data and grab samples, recognized and interpreted positive relief features in the northern middle slope (Domain III) as deep-water coral mounds. Later, in the same region, Maly et al. (2019), based on high-resolution geophysical data, described a W and NW geomorphological positive feature and interpreted it as a carbonate ridge, the Alpha Crucis Carbonate Ridge (ACCR) (Figures 14 and 16), approximately 17 to 11.6 km wide, 100 to 290

m high with a semicircular shape, flanked by an elongated depression, and covered by carbonate sands and gravels overlaid by dead ramified corals. The ACCR occurs in the upper and middle slopes at water depths from 450 to 1250 m (Northeastern domain, III). The authors stated that the ACCR was formed by an upward fluid flow along the salt-related crestal fault at depth and interacted with the IWBC that shapes the bottom and transports coral larvae.

## DISCUSSION

The qualitative and descriptive geomorphological analyses that supported this study provided valuable data for the statistical analysis of PCR-BS environmental data, some of which are described in this special issue. Furthermore, the excellent coverage of the slope and part of the SPP with good-quality 3-D multichannel seismic data enabled us to interpret and describe the geomorphological features on a regional scale and to describe and discuss the interplay between modern morphology and the tectono-sedimentary evolution of the basin, especially from the Palaeogene to the Quaternary.

The modern basin geomorphology relates to four tectono-sedimentary processes: 1) the basement configuration, 2) the presence of the evaporite sequence, 3) the Late Cretaceous uplift of the basin western edge relief (Proto Serra do Mar formation), and 4) the Continental Rift of the Southeastern Brazil formation.

The basement top of the Santos Basin is irregular with occasionally deep areas, especially under the prominent depocenter in the northern-central area (blue area in the map of Figure 1). It also shows basement structural highs, notably in the distal area of the basin in which the External High of the Santos Basin occurs, and structures along the Cretaceous Hinge Line (or Santos Hinge Line) in the western portion of the basin (Figure 2). Slope orientation roughly follows the basement orientation and the Cretaceous Hinge Line design.

Downward and upward salt movements vastly affected the modern seafloor relief. According to Davison et al. (2012), salt movement began in the Early Cretaceous, accelerating due to the Late Cretaceous basin uplift and tilting, which formed the hinge line. The uplift of the basin western edge relief triggered a massive progradation of sediments that

filled the central-northern depocenter and induced salt expulsion to deep waters. The salt diapirs/walls/ridges induced cover sediment deformation by faulting, folding, and crestal collapses that impressed their shape and orientation in the seafloor relief (ridges, minibasins, and crestal

depressions). On its way to deeper waters, salt found a Basement High (External High), which caused a greater rise, printing a peculiar geometry on the seafloor relief that resembles an egg carton (Figure 22), with shallower bathymetries than those in southern-eastern-northern surrounding areas.

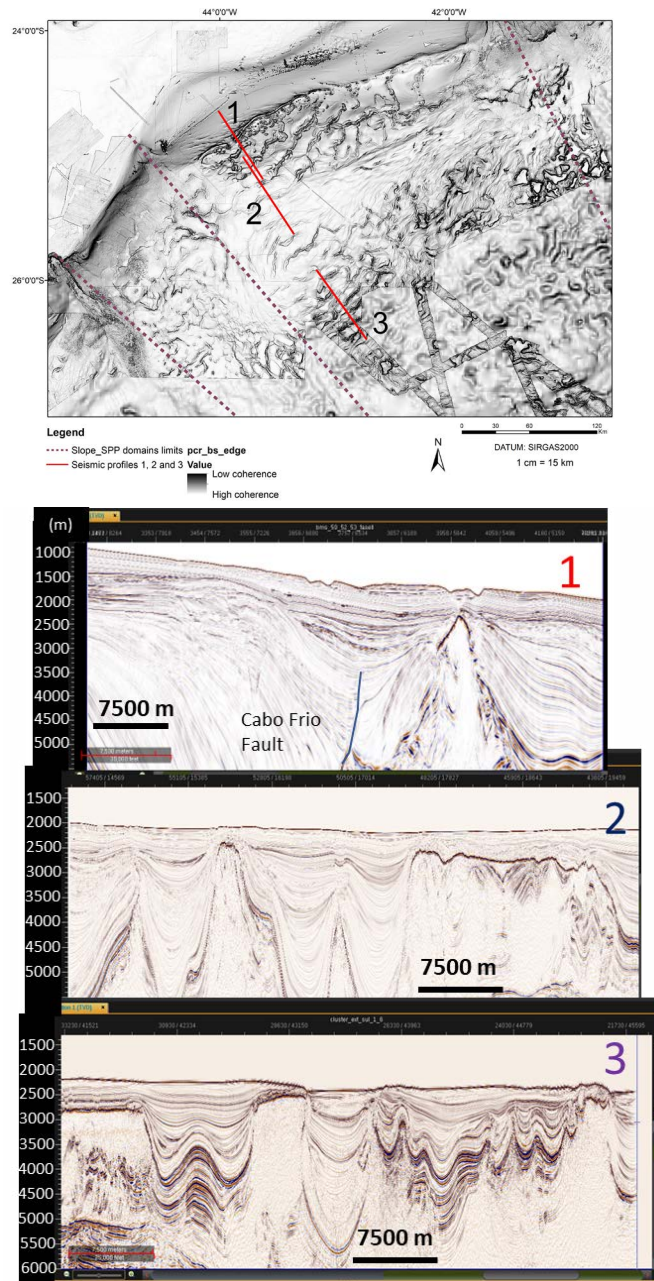


**Figure 22.** Coherence (edge) map with 3 NW-SE seismic profiles (1, 2, and 3, vertical scale in meters) crossing the northeastern geomorphological domain (III) and showing different halotectonic styles, from the Extensional Domain to Salt-Thickened Domain. Profile 1 crosses the limit between the halotectonic domains coinciding with the Cabo Frio fault and the Santos channel on the surface; profile 2 crosses the NE-SW minibasin-ridge-crestal graben region, the São Paulo channel, and a N60E rounded smooth crests and its flanked minibasin; and profile 3 crosses the eastern portion of the Salt-Thickened Domain, which shows shallower diapirs and walls and a rounded disorganized seafloor geomorphic feature.

After the Continental Rift of the Southeastern Brazil installation, the Paraíba do Sul fluvial system moved toward the Campos Basin, decreasing the terrigenous input in the northern Santos Basin and leaving the northern slope and adjacent SPP (Domain III) mostly exposed to the action of ocean bottom currents.

Some authors have noted that oceanographic processes, such as ocean bottom currents and their seafloor interactions, have played an important role in the morphosedimentary process in the continental slope (Mahiques et al., 2022) at least since the late Palaeogene (Duarte and Viana, 2007). Mahiques et al. (2022) indicated that the southward flowing Brazil Current supplies sediments and distributes and erodes the outer shelf and upper slope of the northern portion. They also described sheeted contourites at a water depth below 600 m and associated them with the northeast-flowing IWBC, which gives the seafloor its smooth relief. It is interrupted by the Santos Channel at a water depth of about 1500 m.

On the other hand, in the other domains (I, II, and IV), gravity-driven processes and associated morphologies predominate, such as canyons, ravines, and mass-transport scars and deposits that interact with salt-related relief and faults and ocean bottom currents. Comparing the modern geomorphology of the Santos, Campos, and Espírito Santo basins evinces that the smaller number of canyons in the Santos Basin (only two) indicates a lower sediment transfer from the shelf to the slope-SPP at least during the Late Quaternary.

In Domain I, the salt limit about coincides with the slope-SPP boundary. The SPP contains two well-developed submarine valleys that end in a depocenter. The SPP of Domain II represents a transition between the unsalted zone and the Salt Thickened Domain in the northern portion. Domains I, II, and IV show mass-transport deposits concentrated in the lower slope and SPP and prominent head scars in the upper and middle slopes.

The Santos Basin contains two well-developed pockmark fields in the upper slope terraces of domains I and III and other sparsely distributed occurrences with different bathymetric ranges and associations. In domain I, they are limited by the 1100 m isobath and fail to show well-developed

carbonate pinnacles, as in domain III from 500 to 900 m water depths. Moreover the pockmarks up to 1800 m water depths in the lower slope of domain III are associated with salt-related crestal grabens. One hypothesis refers to a longer lasting exudation in the pockmarks of the northeastern domain.

The possibility of the current activity of these seepages represents an important geohazard but there exists little direct evidence to support this hypothesis. Many seafloor depressions have origins associated with gas hydrate dissociation during glacial lowstand stages, especially at water depths from 500 to 700 m. Hydrate stability depends on pressure and temperature, and thus, vast amounts of methane may be released from melting hydrates during climate change with potentially significant environmental implications (Kennett et al., 2000).

Most likely, the origin of the upper slope pockmark fields is associated with the decomposition of gas hydrates in underlying layers during Pleistocene glacial lowstand stages. However, the sparsely distributed pockmarks on the middle and lower slopes are related to fluid seepages associated with faults at depth and/or carrier beds.

## CONCLUSION

The geomorphology of the continental slope and SPP stems from Quaternary sea-level variations and related gravity-driven depositional processes, sediment reworking by ocean bottom currents, biological processes (bioherms growing), seepages, and underlying salt movements. The regional physiographic province configuration shows a heritage from the basin tectono-sedimentary evolution and basement morphology.

This study divided the slope and the adjacent SPP into four geomorphological domains (I- southwestern, II- central, III- northeastern, and IV- far northeastern) based on their direction, profile, average gradient, shelf break isobath, distribution of the medium-small scale geomorphic features, and the presence or absence of evaporites at subsurface. Downward from each domain, the SPP shows considerable geomorphological variations related to the presence of the evaporite sequence. The boundaries between domains I-II and II-III contain the Cananéia and São Sebastião canyons,

respectively. Domains I and III show upper slope terraces and convex/linear profiles, and domains II and IV have concave/exponential profiles.

Upward and downward salt movements have vastly affected the modern seafloor relief of the continental slope (domains I and III, downward the Cabo Frio fault) and the SPP of the central (II) and northeastern (III) domains. The salt diapirs/walls/ridges have induced cover sediment deformation by faulting, folding, and crestal collapses that impressed their shape and orientations on the seafloor relief (ridges, minibasins, and crestal depressions).

The southwestern, central, and far northeastern domains include mass-transport complexes and associated features (headscarp, scars, and rugous seafloor relief), unlike the northeastern domain, whose slope and SPP, up to the 2200 m isobath, were reworked and shaped by ocean bottom currents, and the mass-transport deposits are characterized by localized occurrences, smaller dimensions, and runouts. Moreover, the upper and middle southwestern slopes show some features (reshaped depressions) related to ocean bottom current action, probably the IWBC.

The Santos Basin contains two well-developed pockmark fields in domains I and III, with different bathymetric ranges and associations. In domain III, pockmark fields occur at water depths from 500 to 900 m, some of which contain well-developed carbonate pinnacles. Furthermore, they occur up to 1800 m water depths, associated with salt crests and crestal grabens. In contrast, the pockmarks in domain I are limited by the 1100 m isobath.

Little direct evidence can support the hypothesis about the pockmarks current activity. Many seafloor depressions, such as pockmarks, have their origins associated with gas hydrate dissociation during glacial lowstand stages, especially at water depths from 500 to 700 m. It is likely that the upper slope pockmark fields originated during a Pleistocene lowstand stage. Moreover, one hypothesis to explain carbonate pinnacles associated with pockmarks may refer to a longer lasting exudation (fluid seepage) in some pockmarks of the northeastern middle slope, which are associated with faults at depth and/or carrier beds.

## ACKNOWLEDGMENTS

We would like to thank PETROBRAS for providing data and granting permission to publish this study, PCR-BS coordinator Daniel Leite Moreira for his support, and the anonymous reviewers for their comments and valuable contributions.

## AUTHOR CONTRIBUTIONS

C.M.H.: Conceptualization, Investigation and Writing – original draft; Writing – review & editing.

S.S.: Methodology; seismic mapping; Investigation; review & editing.

E.T.I.F.: Methodology; GIS Analysis, editing.

## REFERENCES

- Brown, A. R. 2004. *Interpretation of three-dimensional seismic data* (5th ed). Tulsa: AAPG Memoir 42.
- Bueno, G. V., Machado, D. L. JR, Oliveira, J. A. B. & Marques, E. J. J. 2004. A influência do Lineamento Capricórnio na evolução tectono-sedimentar da Bacia de Santos. In: *Congresso Brasileiro de Geologia* (52th ed, p. 733). Araxá: Sociedade Brasileira de Geologia. <http://www.sbgeo.org.br/home/pages/33>, accessed in November 2022.
- Carvalho, N. F., Waters, L. G., Arantes, R. C. M., Couto, D. M., Cavalcanti, G. H., Güth, A. Z., Falcão, A. P. C., Nagata, P. D. P., Hercos, C. M., Sasaki, D. K., Dottori, M., Cordes, E. E & Sumida, P. Y. G., 2023. Underwater surveys reveal deep-sea corals in newly explored regions of the southwest Atlantic. *Communications Earth & Environment* 4, 282.
- Davison, I., Anderson, L. & Nuttall, P., 2012. Salt deposition, loading and gravity drainage in the Campos and Santos salt basins. In: Alsop, G.I., Archer, S.G., Hartley, A.J., Grant, N.T., Hodgkinson, R. (eds.), *Salt Tectonics, Sediments and Prospectivity*, 363, (pp. 159–174). London: Geological Society of London, Spec. Pub.
- Duarte, C. S. L. & Viana, A. R. 2007. Santos Drift System: stratigraphic organization and implications for late Cenozoic palaeocirculation in the Santos Basin, SW Atlantic Ocean. In: Viana, A. R. & Rebesco, M. (eds.), *Economic and Palaeoceanographic Significance of Contourite Deposits* (pp. 171-198). London: Geological Society of London.
- Ericson, C. & Wollin, G. 1968. Pleistocene climates and chronology in deep-sea sediments. *Science*, 16, 1227-1234.
- Gamboa, L. A. P., Pinheiro Machado, M. A., Silveira, D. P., Freitas, J. T. R. & Silva, R. P. 2008. Evaporitos estratificados no Atlântico Sul: Interpretação sísmica e controle tectono-estratigráfico na Bacia de Santos. In: Mohriak, W., Szatmari, P. & Anjos, S. M. C. (Eds.). *Sal, Geologia e Tectônica*. Exemplos nas Bacias Brasileiras (pp. 343-361). São Paulo: Beca.
- Gardner, M. H., Borer, J. M., Romans, B. W., Baptista, N., Kling, E. K., Hanggoro, D., Melick, J. J., Wagerle, R. M., Dechesne, M., Carr, M. M., Amerman, R. & Atan, S.

2008. *Stratigraphic Models for Deep-Water Sedimentary Systems*. In: 28th Annual Gulf Coast Section SEPM. Houston: SEPM.
- Imbrie, J. 1985. A theoretical framework for the Pleistocene ice ages. *Journal of Geological Society*, 142, 417-432.
- Jackson, C. A. L., Jackson, M. P. A., Hudec, M. R. & Rodriguez, C. R. 2015. Enigmatic structures within salt walls of the Santos Basin – part 1: Geometry and kinematics from 3D seismic reflection and well data. *Journal of Structural Geology*, 75, 135-162.
- Kennett, J. P., Cannariato, K. G., Hendy, I. L. & Behl, R. J. 2000. Carbon Isotopic Evidence for Methane Hydrate Instability during Quaternary Interstadials, *Science*, 288, 128-133.
- Lee, G., Lee, K. & Kim, H. 2009. Effects' Impact on Seismic Search and Discovery. *AAPG Explorer*, (40474).
- Mahiques, M. M., Schattner, U., Lazar, M., Sumida, P. Y. G. & Souza, A. P. 2017. An extensive pockmark field on the upper Atlantic margin of Southeast Brazil: spatial analysis and its relationship with salt diapirism. *Helyon*, 3, e00257.
- Mahiques, M. M., Lobo, F. J., Schattner, U., Lopez-Quir, A., Rocha, C. B., Dias, R. J. S., Montoya-Montes, I. & Vieira, A. C. B. 2022. Geomorphological imprint of opposing ocean bottom currents, a case study from the southeastern Brazilian Atlantic margin. *Marine Geology*, 444, 106715.
- Maly, M., Schattner, U., Lobo, F., Ramos, R. B., Dias, R. J., Couto, D. M., Sumida, P. Y. & Mahiques, M. M., 2019. The Alpha Crucis Carbonate Ridge (ACCR): Discovery of a giant ring-shaped carbonate complex on the SW Atlantic margin. *Scientific Reports*, 9, 18697.
- Meisling, E., Cobbold, P. R. & Mount, V. S., 2001. Segmentation of an obliquely rifted margin, Campos and Santos basins, southeastern Brazil. *AAPG Bulletin*, 85 (11), 1903–1924.
- Modica, C. J. & Brush, E. R. 2004. Post rift sequence stratigraphy, paleogeography, and fill history of the deep-water Santos Basin, offshore southeast Brazil. *AAPG Bulletin*, 88(7), 923-945.
- Mohriak, W. U., Macedo, J. M., Castellani, R. T., Rangel, H. D., Barros, A. Z. N., Latgé, M. A. L., Ricci, J. A., Mizusaki, A. M. P., Szatmari, P., Demercian, L.s., Rizzo, J. G. & Aires, J. R. 1995. Salt Tectonics and structural styles in deep-water province of Cabo Frio region, Rio de Janeiro, Brazil. In: Jackson, M. P. A., Roberts, D. G. & Snelson, S. (eds.), *Salt Tectonics: A global perspective*: American Association of Petroleum (pp. 273-304). Tulsa: AAPG.
- Moreira, J. L. P., Madeira, C. V., Gil, J. A. & Machado, M. A. P. 2007. Bacia de Santos. *Boletim de Geociências da Petrobras*, 15(2), 531-549.
- Ramos, R. B., Santos, R. F., Schattner, U., Figueira, R. C. L., Bicego, M. C., Lobo, F. J. & Mahiques, M. M. 2019. Deep pockmarks as natural traps: a case study from Southern Santos Basin (SW Atlantic upper slope). *Geo-Marine Letters*, 40, 989-999.
- Riccomini, C. 1991. *O Rift Continental do Sudeste do Brasil*. (phd dissertation) Universidade de São Paulo. <https://www.teses.usp.br/teses/disponiveis/44/44136/tde-18032013-105507/pt-br.php>, accessed in November 2022.
- Rowan, M. G., Tilton, J., Lebit, H. & Fiduk, J. C. 2022. Thin-skinned extensional salt tectonics, counterregional faults, and the Albian Gap of Brazil. *Marine and Petroleum Geology*, 137, 10547.
- Schattner, U., Lazar, M., Souza, L. A. P., Brink, U. T. & Mahiques, M. M. 2016. Pockmarks asymmetry and seafloor currents in the Santos Basin offshore Brazil. *Geo-Marine Letters*, 36, 457-464.
- Schattner, U., Lobob, F. J., García, M., Kanari, M., Ramos, R. B. & Mahiques, M. M. 2018. A detailed look at diapir piercement onto the ocean floor: New evidence from Santos Basin, offshore Brazil. *Marine Geology*, 406, 98-108.
- Schreiner, S., Souza, M. B. F. M. & Migliorelli, J. P. R. 2009. Modelo digital da geomorfologia do fundo oceânico do centro-sul da Bacia do Espírito Santo e norte da Bacia de Campos. *Boletim de Geociências da Petrobras*, 17 (2), 365-369.
- Sharp, A. & Badalini, G. 2013. Using 3D seismic data to map shallow-marine geohazards: a case study from the Santos Basin, Brazil. *Petroleum Geoscience*, 19, 157-167.
- Silveira, I. C. A., Lazaneo, C. Z., Amorim, J. P. M., Silva, M. B., Bernardo, P. S., Martins, R. C., Santos, D. M. C., Dottori, M., Belo, W. C., Martins, R. P. & Moreira, D. L. 2022. Oceanographic conditions of the continental slope and deep waters in Santos Basin: the SANSED cruise (winter 2019). *Ocean and Coastal research*, 71(Supl.3).
- Souza, K. G. 1991. *La marge continentale bresilienne sub-orientale et les domaines ocdaniques adjacents: structure et dvolution*. (PhD dissertation). Université Pierre et Marie Curie. <https://www.theses.fr/1991PA066138>, accessed in November 2022.
- Viana, A. R. & Faugeres, J. C. 1998. Upper slope sand deposits: the example of Campos Basin, a latest Pleistocene/Holocene record of the interaction between along-slope and downslope currents. In: Stoker, M. S., Evans, D. & Cramp, A. (eds) *Geological Processes on Continental Margins: Sedimentation, Mass-Wasting and Stability* (pp. 287-316). London: Geological Society.
- Viana, A. R., Hercos, C. M., Almeida Jr, W., Magalhães, J. L. C. & Andrade, S. B. 2002. Evidence of bottom current influence on the Neogene to Quaternary sedimentation along the northern Campos slope, SW Atlantic margin. In: Stow, D. A. V., Faugeres, J.-C., Howe, J. A., Pudsey, C. J. & Viana, A. R. (eds.), *Deep-Water Contourite Systems: Modern Drifts and Ancient Series, Seismic and Sedimentary Characteristics* (pp. 249-259). London: Geological Society.
- Vivalvi, M. A. 1997. Zoneamento bioestratigráfico e paleoclimático dos sedimentos do Quaternário Superior do talude da Bacia de Campos. *Boletim de Geociências da PETROBRAS*, 11 (1/2), 132-165.